

Online Appendix to “What explains international interest rate co-movement?”

Annika Camehl* Gregor von Schweinitz†

September 4, 2023

*Department of Econometrics, Erasmus University Rotterdam, Burgemeester Oudlaan 50, 3062 PA Rotterdam, The Netherlands, camehl@ese.eur.nl

†Halle Institute for Economic Research and Leipzig University, Kleine Märkerstr. 8, D-06108 Halle (Saale), Germany, Gregorvon.Schweinitz@iwh-halle.de

A Data

Table A.1: Data

Variable	Description
baseline VAR variables	
y	output gap; source: Oxford Economics, datastream codes AUXOGAP.R, CNXOGAP.R, EKXOGAP.R, JPXOGAP.R, KOXOGAP.R, UKXOGAP.R, USXOGAP.R
π	year-on-year inflation rate calculated from consumer prices (all items); source: IMF-IFS and Eurostat, Datastream codes AUI64...F, CNI64...F, EMCONPRCF, JPI64...F, KOI64...F, UKI64...F, USI64...F
r	quarterly average of monthly policy rates and Krippner shadow rates; sources: https://www.ljkmfa.com/ and national central banks, Datastream codes (dates of shadow rate) AUPRATE., CNB14044, EMREPO.. (02/2009-12/2019), JPPRATE. (05/1995-12/2019), KOI60B.., UKPRATE. (12/2008-10/2017), FREFEDFD (11/2008-07/2016)
σ	real effective exchange rate (narrow), defined as nominal effective exchange rate times the ratio of a weighted sum of foreign price indices relative to a domestic price index; source: BIS (we are using the inverse of the data), https://www.bis.org/statistics/eer.htm
Variables for VAR extensions	
sp	stock prices, yoy growth rates; source: Thomson Reuters, Datastream codes: AUSHRPRCF, CN-SHRPRCF, EMSHRPRCF, JPSHRPRCF, KOSHPRRCF, UKSHRPRCF, USSHRPRCF
ts	term spread, long-term bond yields minus r ; source (bond yields): Thomson Reuters, Datastream codes AUGBOND., CNGBOND., EMGBOND., JPGBOND., KOGBOND., UKGBOND., USGBOND.
exp	exports, % GDP; source: OECD Quarterly National Accounts, Oxford Economics, Datastream codes: AUOEXP01D, CNOEXP01D, EKXMSA..D, JPOEXP01D, KOOEXP01D, UKOEXP01D, USO-EXP01D
imp	imports, % GDP; source: OECD Quarterly National Accounts, Oxford Economics, Datastream codes: AUOEXP05D, CNOEXP05D, EKXXSA..D, JPOEXP05D, KOOEXP05D, UKOEXP05D, USO-EXP05DF
$trade$	sum of exports and imports, % GDP
$GDP(real)$	numerator for $exp, imp, trade$; source: OECD Quarterly National Accounts, Oxford Economics, Datastream codes: AUOEXP03D, CNOEXP03D, EKXGDSA.D, JPOEXP03D, KOOEXP03D, UKOEXP03D, USOEXP03D
Foreign weights	
trade weights	BIS trade weights averaged over 1980 to 2019 (narrow), source: BIS, https://www.bis.org/statistics/eer.htm . The Bilateral weights are reported for three-year periods and are quite stable over time. We take the average over all three-year blocks in our sample period, and normalize bilateral weights in our restricted sample of seven countries to sum up to 1.
bank weights:	BIS data on total liabilities of the locational banking statistics, https://www.bis.org/statistics/bankstats.htm?m=2069
bank weights:	BIS data on total claims of the locational banking statistics, https://www.bis.org/statistics/bankstats.htm?m=2069
LBS claims	
bank weights:	BIS data on the consolidated banking statistics, https://www.bis.org/statistics/consstats.htm?m=2070
CBS	
External instruments, used to cross-check with global shocks	
BH	Median of oil supply shocks identified from Baumeister and Hamilton (2019) , updated to December 2022, https://sites.google.com/site/cjsbaumeister/research
Ksurp	monthly oil supply surprise shocks from Käenzig (2021) , updated to December 2022, https://github.com/dkaenzig/oilsupplynews
Knews	monthly oil supply news shocks from Käenzig (2021) , updated to December 2022, https://github.com/dkaenzig/oilsupplynews
JQ	Innovations to the financial conditions index of Jermann and Quadrini (2012) as used in Mumtaz et al. (2018)
EBP	Excess bond premium of Gilchrist and Zakrajšek (2012) as used in Mumtaz et al. (2018)
NEWS	Textual proxy for credit supply shocks, from Mumtaz et al. (2018)

B Theoretical model for identifying restrictions

Following Lubik and Schorfheide (2007), we consider a model with an international Phillips curve, IS curve, monetary policy rule, and (real) exchange rate equation, to which we add common shifts of country-specific supply and demand curves in the form of global supply and demand shocks. The set of equations for country $c \in \{1, \dots, C\}$ is given by:

$$y_{ct} = \frac{\tilde{\tau}^c}{\kappa^c} \left[\mu^{c,s} + \pi_{ct} - \beta^c E[\pi_{ct+1}] + \frac{\alpha^c \beta^c}{1 - \alpha^c} E[\sigma_{ct+1}] - \frac{\alpha^c}{1 - \alpha^c} \sigma_{ct} \right] + \chi_c^s u_{gt}^s + u_{ct}^s \quad (\text{B.1})$$

$$y_{ct} = \mu^{c,d} + E[y_{ct+1}] - \tilde{\tau}^c (r_{ct} - E[\pi_{ct+1}]) + \alpha^c (2 - \alpha^c) \frac{1 - \tau^c}{\tau^c} E[y_{ct+1}^*] + \dots \quad (\text{B.2})$$

$$+ \frac{\alpha^c \tilde{\tau}^c}{1 - \alpha^c} E[\sigma_{ct+1}] + \chi_c^d u_{gt}^d + u_{ct}^d$$

$$r_{ct} = \rho^c r_{it-1} + (1 - \rho^c) [(\psi^{c,1} + \psi^{c,3}) \pi_{ct} + \psi^{c,2} y_{ct} + \psi^{c,3} (\sigma_{ct} - \pi_{ct}^*)] + u_{ct}^m \quad (\text{B.3})$$

$$\sigma_{ct} = \mu^{c,\sigma} - \frac{1 - \alpha^c}{\tilde{\tau}^c} (y_{ct}^* - y_{ct}) + u_{ct}^\sigma \quad (\text{B.4})$$

with

$$\tilde{\tau}^c = \tau^c + \alpha^c (2 - \alpha^c) (1 - \tau^c), \quad y_{ct}^* = \sum_{c^* \neq c} w_{cc^*} y_{c^*t}, \quad \pi_{ct}^* = \sum_{c^* \neq c} w_{cc^*} \pi_{c^*t},$$

Equation (B.1) expresses the open economy Phillips curve. Supply depends on inflation and changes in the exchange rate. The parameter α^c , $0 < \alpha^c < 1$, measures the import share. When $\alpha^c = 0$, the model reduces to a closed economy set-up. τ^c gives the intertemporal substitution elasticity, β^c the discount factor, and κ^c the slope coefficient of the Phillips curve.

Equation (B.2) models the open economy IS curve. Demand is expressed as a function of interest rates, inflation, foreign output, and changes in the exchange rate. We substitute expectations in equations (B.1) and (B.2) with simple autoregressive forecasts, following Baumeister and Hamilton (2018). We model the expected value of a variable z as $z_{t+1|t} = c^z + \phi^z z_{t|t}$. We set the autoregressive parameter equal for all variables, as $\phi^c = 0.75$.¹ The term c^z is absorbed in the constant terms. The parameter ζ^c weights expected output in the IS curve. The Phillips and IS curve can then be expressed as

$$y_{ct} = \frac{\tilde{\tau}^c}{\kappa^c} \left[\mu^{c,s} + (1 - \beta^c \phi^c) \left[\pi_{ct} - \frac{\alpha^c}{1 - \alpha^c} \sigma_{ct} \right] \right] + u_{ct}^s \quad (\text{B.5})$$

$$y_{ct} = \frac{1}{1 - \zeta^c \phi^c} \left[\mu^{c,d} - \tilde{\tau}^c (r_{ct} - \phi^c \pi_{ct}) + \alpha^c (2 - \alpha^c) \frac{1 - \tau^c}{\tau^c} (\phi^c - 1) y_{ct}^* + \frac{\alpha^c \tilde{\tau}^c \phi^c}{1 - \alpha^c} \sigma_{ct} \right] + u_{ct}^d \quad (\text{B.6})$$

¹Note that Lubik and Schorfheide (2007) include in some equations expected changes in variables (as opposed to expected values of the variables). In such cases, we model the expected value of a change in variable z_{t+1} , denoted by $E(\Delta z_{t+1}) = (0.75 - 1)z_t$.

The monetary policy authority sets interest rates according to the rule given in equation (B.3). The parameter $\psi^{c,1}$ captures the response of the monetary policy authority to changes in inflation, $\psi^{c,2}$ reflects the reaction to output, and $\psi^{c,3}$ to changes in the nominal exchange rate. ρ^c is a smoothing parameter, smoothing the implementation of monetary policy over time. Equation (B.4) relates changes in the exchange rate to differences in foreign and domestic output. We use that under PPP [Lubik and Schorfheide \(2007\)](#) express inflation as $\pi_{ct} = ex_{ct} + (1 - \alpha^c)q_{ct} + \pi_{ct}^*$ where ex_{ct} are changes in the nominal exchange rate and q_{ct} changes in terms of trade. Thus, the real exchange rate relates to terms of trades as $q_{ct} = -\frac{1}{1-\alpha^c}\sigma_{ct}$.

Our coefficients in the panel SVAR model given in equations (AS) to (ER) are related to the structural parameters in the theoretical model in the following way:

$$\begin{aligned}\alpha^{c,\pi} &= \frac{\tilde{\tau}^c}{\kappa^c}(1 - \beta^c\phi^c), \quad \alpha^{c,\sigma} = -\frac{\tilde{\tau}^c}{\kappa^c}(1 - \beta^c\phi^c)\frac{\alpha^c}{1 - \alpha^c} \\ \beta^{c,r} &= -\frac{1}{1 - \zeta^c\phi^c}\tilde{\tau}^c, \quad \beta^{c,\pi} = \frac{1}{1 - \zeta^c\phi^c}\tilde{\tau}^c\phi^c \\ \beta^{c,y^*} &= \frac{1}{1 - \zeta^c\phi^c}\alpha^c(2 - \alpha^c)\frac{1 - \tau^c}{\tau^c}(\phi^c - 1), \quad \beta^{c,\sigma} = \frac{1}{1 - \zeta^c\phi^c}\frac{\alpha^c\tilde{\tau}^c\phi^c}{1 - \alpha^c} \\ \psi^{c,\pi} &= \psi^{c,1} + \psi^{c,3}, \quad \psi^{c,y} = \psi^{c,2}, \quad \psi^{c,\sigma} = \psi^{c,3} \\ \theta^{c,y} &= \frac{1 - \alpha^c}{\tilde{\tau}^c}.\end{aligned}$$

C Econometric model

As our baseline, we estimate a Bayesian structural panel VAR with global shocks using $J = 4$ variables from a panel of $C = 7$ countries:

$$\begin{aligned}\mathbf{Ay}_t &= \mathbf{Bx}_{t-1} + \chi\mathbf{u}_{gt} + \mathbf{u}_t \\ \mathbf{u}_t &\sim \mathcal{N}(\mathbf{0}, \mathbf{D}), \quad \mathbf{u}_{gt} \sim \mathcal{N}(\mathbf{0}, \mathbf{I}_G).\end{aligned}$$

The model has $n = CJ$ equations, jointly indexed by subscript $c \in \{1, \dots, C\}$ and superscript $j \in \{s, d, m, \sigma\}$. The vector $\mathbf{u}_{gt} = (u_{gt}^s, u_{gt}^d)$ contains $G = 2$ global shocks (which are related to a subset of the J structural equations), which load onto structural equation j in country c according to the loadings χ_c^j stacked in the $n \times G$ loading matrix χ :

$$\chi = \left[\begin{pmatrix} \text{diag}(\chi_1) \\ \mathbf{0}_{J-G \times G} \end{pmatrix}' \quad \begin{pmatrix} \text{diag}(\chi_2) \\ \mathbf{0}_{J-G \times G} \end{pmatrix}' \quad \dots \quad \begin{pmatrix} \text{diag}(\chi_C) \\ \mathbf{0}_{J-G \times G} \end{pmatrix}' \right]'$$

with $\chi_c = (\chi_c^s, \chi_c^d)$.

Conditional on realized global shocks \mathbf{u}_{gt} , the model is identical to a standard Bayesian

structural VARX with global shocks as exogenous variables:

$$\begin{aligned}\mathbf{A}\mathbf{y}_t &= \mathbf{B}\mathbf{x}_{t-1} + \chi\mathbf{u}_{gt} + \mathbf{u}_t \\ &= [\mathbf{B} \quad \chi] \begin{bmatrix} \mathbf{x}'_{t-1} & \mathbf{u}'_{gt} \end{bmatrix}' + \mathbf{u}_t\end{aligned}$$

This implies that we can formulate a joint prior for \mathbf{B} and χ , and derive a joint posterior distribution for these parameters. Furthermore, because of the orthogonality of structural domestic shocks u_{ct}^j , the model can be estimated equation-by-equation, conditional on structural contemporaneous coefficients \mathbf{A} and global shocks \mathbf{U}_{gt} (Baumeister and Hamilton, 2015).

Let \mathbf{a}_c^j and \mathbf{b}_c^j be the $(1 \times n)$ - and $(1 \times k)$ -dimensional row vectors of structural coefficients (contemporaneous and lagged) in the j^{th} structural equation of country c and d_c^j the variance of the corresponding structural domestic shocks. If we include a structural global shock u_{gt}^j for equation j , χ_c^j denotes the loading onto country c . That is, the structural equation $j \in \{s, d\}$ in country c is

$$\begin{aligned}\mathbf{a}_c^j \mathbf{y}_t &= \mathbf{b}_c^j \mathbf{x}_{t-1} + \chi_c^j u_{gt}^j + u_{ct}^j \\ u_{ct}^j &\sim \mathcal{N}(0, d_c^j), \quad u_{gt}^j \sim \mathcal{N}(0, 1).\end{aligned}$$

The structural equations without a global shock, $j \in \{m, \sigma\}$, reduce to

$$\mathbf{a}_c^j \mathbf{y}_t = \mathbf{b}_c^j \mathbf{x}_{t-1} + u_{ct}^j, \quad u_{ct}^j \sim \mathcal{N}(0, d_c^j).$$

C.1 Restrictions on structural parameters

We impose homogeneity restrictions on \mathbf{a}_c^j and \mathbf{b}_c^j such that foreign coefficients are identical up to a scaling constant w_{cc^*} . That is, instead of one coefficient per variable and foreign country (contemporaneous or lagged), we estimate a single coefficient on the same foreign variable, but aggregated over countries. This coefficient is then distributed to the individual countries according to aggregation weights w_{cc^*} . The homogeneity restrictions allow us to reduce the dimensionality of the problem by working with coefficient vectors $\tilde{\mathbf{a}}_c^j$ and $\tilde{\mathbf{b}}_c^j$ instead, which are of dimension $(1 \times 2J)$ and $(1 \times \tilde{k})$, respectively (with $\tilde{k} = 2Jp + 2$). The homogeneity restrictions can be written as

$$\mathbf{a}_c^j = \tilde{\mathbf{a}}_c^j \mathbf{R}_c^A \tag{C.1}$$

$$\mathbf{b}_c^j = \tilde{\mathbf{b}}_c^j \mathbf{R}_c^B. \tag{C.2}$$

The restricted vector $\tilde{\mathbf{a}}_c^j$ first contains J domestic coefficients and then J foreign coefficients. The $2J \times n$ restriction matrix \mathbf{R}_c^A applies the appropriate scaling and allocates them to the

right position in $\tilde{\mathbf{a}}_c^j$ and is therefore defined as

$$\mathbf{R}_c^A = \begin{pmatrix} \mathbf{0}_{J \times J} & \cdots & \mathbf{0}_{J \times J} & \mathbf{I}_J & \mathbf{0}_{J \times J} & \cdots & \mathbf{0}_{J \times J} \\ w_{c,1}\mathbf{I}_J & \cdots & w_{c,c-1}\mathbf{I}_J & \mathbf{0}_{J \times J} & w_{c,c+1}\mathbf{I}_J & \cdots & w_{c,C}\mathbf{I}_J \end{pmatrix}_{(2J \times n)}.$$

Restricted structural lag coefficients $\tilde{\mathbf{b}}_c^j$ use the same ordering as $\tilde{\mathbf{a}}_c^j$ for every lag. The restriction matrix \mathbf{R}_c^B is a block-diagonal matrix with \mathbf{R}_c^A for every lag, and an identity matrix for the constant and trend:

$$\mathbf{R}_c^B = \begin{pmatrix} \mathbf{R}_c^A & \mathbf{0}_{2J \times n} & \cdots & \cdots & \mathbf{0}_{2J \times n} & \mathbf{0}_{2J \times 2} \\ \mathbf{0}_{2J \times n} & \mathbf{R}_c^A & \mathbf{0}_{2J \times n} & \cdots & \mathbf{0}_{2J \times n} & \mathbf{0}_{2J \times 2} \\ \vdots & \vdots & \ddots & \vdots & \vdots & \vdots \\ \mathbf{0}_{2J \times n} & \cdots & \cdots & \cdots & \mathbf{R}_c^A & \mathbf{0}_{2J \times 2} \\ \mathbf{0}_{2 \times n} & \cdots & \cdots & \cdots & \mathbf{0}_{2 \times n} & \mathbf{I}_{2 \times 2} \end{pmatrix}_{(\tilde{k} \times k)}.$$

As an example, let us look at the structural contemporaneous coefficients in the first four equations, which correspond to Australia. Combining the four row vectors into one 4×8 -matrix $\tilde{\mathbf{A}}_{AU}$, our baseline model identifies

$$\tilde{\mathbf{A}}_{AU} = \begin{pmatrix} 1 & -\alpha^{AU,\pi} & 0 & \alpha^{AU,\sigma} & 0 & 0 & 0 & 0 \\ \frac{1}{-(1-\rho^{AU})\psi^{AU,y}} & -\beta^{AU,\pi} & -\beta^{AU,r} & -\beta^{AU,\sigma} & -\beta^{AU,y^*} & 0 & 0 & 0 \\ -\theta^{AU,y} & -(1-\rho^{AU})\psi^{AU,\pi} & 1 & -(1-\rho^{AU})\psi^{AU,\sigma} & 0 & (1-\rho^{AU})\psi^{AU,\sigma} & 0 & 0 \\ 0 & 0 & 0 & 1 & \theta^{AU,y} & 0 & 0 & -\theta^{AU,\sigma^*} \end{pmatrix}.$$

Multiplying $\tilde{\mathbf{A}}_{AU}$ with the restriction matrix \mathbf{R}_{AU}^a returns the first four rows of \mathbf{A} . Proceeding similarly for every other country returns the full matrix \mathbf{A} , which can then be used to evaluate the posterior distribution described below.

Note that for the four equations corresponding to the same country c we can apply the restriction matrices $\mathbf{R}_c^A, \mathbf{R}_c^B$ equivalently to the data, i.e.:

$$\begin{aligned} \mathbf{A}_c \mathbf{y}_t &= \mathbf{B}_c \mathbf{x}_{t-1} + \begin{pmatrix} \text{diag}(\chi_c) \\ \mathbf{0}_{J-G \times G} \end{pmatrix} \mathbf{u}_{gt} + \mathbf{u}_{ct} \\ \Leftrightarrow \tilde{\mathbf{A}}_c (\mathbf{R}_c^A \mathbf{y}_t) &= \tilde{\mathbf{B}}_c (\mathbf{R}_c^B \mathbf{x}_{t-1}) + \begin{pmatrix} \text{diag}(\chi_c) \\ \mathbf{0}_{J-G \times G} \end{pmatrix} \mathbf{u}_{gt} + \mathbf{u}_{ct} \\ \Leftrightarrow \tilde{\mathbf{A}}_c \tilde{\mathbf{y}}_{ct} &= \tilde{\mathbf{B}}_c \tilde{\mathbf{x}}_{c,t-1} + \begin{pmatrix} \text{diag}(\chi_c) \\ \mathbf{0}_{J-G \times G} \end{pmatrix} \mathbf{u}_{gt} + \mathbf{u}_{ct} \end{aligned}$$

C.2 Prior distributions for lag coefficients, loadings and domestic shock variances

The full prior distribution of our structural PVAR model with global shocks largely follows [Baumeister and Hamilton \(2018\)](#), and can be written as

$$p(\mathbf{A}, \mathbf{B}, \mathbf{D}, \boldsymbol{\chi}, \mathbf{U}_{gT}) = p(\mathbf{A})p(\mathbf{D}|\mathbf{A})p(\mathbf{B}, \boldsymbol{\chi}|\mathbf{A}, \mathbf{D})p(\mathbf{U}_{gT}). \quad (\text{C.3})$$

The prior distribution of \mathbf{A} is described above, and the global shocks \mathbf{u}_{gt} are independently standard-normally distributed. As in [Baumeister and Hamilton \(2018\)](#), we condition on \mathbf{A} to formulate a normal-inverse gamma prior distribution for the remaining coefficients in each structural equation $(\mathbf{b}_c^j, \chi_c^j, d_c^j)$:

$$\begin{aligned} p((d_c^j)^{-1}|\mathbf{A}) &\sim \Gamma(\tau_c^j, \kappa_c^j) \\ p((\mathbf{b}_c^j, \chi_c^j)|\mathbf{A}, d_c^j) &\sim \mathcal{N}(\mathbf{m}_c^j, d_c^j \mathbf{M}_c^j) \end{aligned}$$

The priors come from a Minnesota prior conditional on \mathbf{A} , using the variance matrix \mathbf{S} of univariate autoregressions of the elements of \mathbf{y}_t . That is, (d_c^j) follows a gamma distribution with mean $1/(\mathbf{a}_c^j \mathbf{S}(\mathbf{a}_c^j)')$, and a prior weight of $\kappa_c^j = 2$. The prior mean \mathbf{m}_c^j of the conditional normal distribution combines (a) the prior belief that the data follow an AR(1) process with AR-coefficient $\phi = 0.75$, and (b) that the central bank engages in interest-rate smoothing, as described by the structural coefficient ρ^c . The first prior implies that the elements of the first lag in \mathbf{b}_c^j should be close to $\phi \mathbf{a}_c^j$, while later lags are centered around 0, with increasing confidence on these priors for higher lags. The exact specification of the Minnesota prior is identical to [Baumeister and Hamilton \(2018\)](#). The second belief is modeled by an additional prior, which centers the first lag of domestic interest rates in the monetary policy equation around the corresponding smoothing coefficient ρ^c . This prior has a variance $V_c^j = 0.1$. If the structural equation contains a global shock, the last element of \mathbf{m}_c^j and \mathbf{M}_c^j contains a prior mean of zero and a variance of ten (to be further scaled by d_c^j) of the global shock loading χ_c^j .

Note that the prior of zero for foreign coefficients in \mathbf{x}_{t-1} is consistent with the homogeneity restrictions formulated above. That is, we formulate the following prior for

restricted lag coefficients $\tilde{\mathbf{b}}_c^j$ and loading χ_c^j :

$$\begin{aligned}
p((\tilde{\mathbf{b}}_c^j, \chi_c^j) | \mathbf{A}, d_c^j) &\sim \mathcal{N}(\tilde{\mathbf{m}}_c^j, d_c^j \tilde{\mathbf{M}}_c^j) \\
\tilde{\mathbf{m}}_c^j &= \mathbf{m}_c^j \left(\tilde{\mathbf{R}}_c^B \right)' \\
\tilde{\mathbf{M}}_c^j &= \tilde{\mathbf{R}}_c^B \mathbf{M}_c^j \left(\tilde{\mathbf{R}}_c^B \right)' \\
\tilde{\mathbf{R}}_c^B &= \begin{pmatrix} \mathbf{R}_c^B & \mathbf{0}_{\tilde{k} \times 1} \\ \mathbf{0}_{1 \times k} & 1 \end{pmatrix}
\end{aligned}$$

C.3 Posterior distributions and algorithm

Drawing the latent global shocks requires an additional Gibbs sampler step compared to [Baumeister and Hamilton \(2015\)](#). However, we show that – conditional on \mathbf{U}_{gT} – the derivation of [Baumeister and Hamilton \(2015\)](#) for the posterior of \mathbf{A} also hold under our homogeneity restrictions.

Let the $(T \times n)$ -dimensional matrix $\mathbf{Y} = (\mathbf{y}_1, \dots, \mathbf{y}_T)'$ and $(T \times k)$ -dimensional matrix $\mathbf{X} = (\mathbf{x}_0, \dots, \mathbf{x}_{T-1})'$ collect all observations. For country c and structural equation j , we construct extended data $\tilde{\mathbf{Y}}_c^j$ and $\tilde{\mathbf{X}}_c^j$ by applying three data modifications. First, we account for the homogeneity restrictions by multiplying \mathbf{X} with the appropriate restriction matrix. Second, if the structural equation contains a global shock, we condition on the j^{th} global shock \mathbf{U}_{gT}^j , which we append as an additional data series once we obtained a posterior draw. Third, we condition on the appropriate row \mathbf{a}_c^j of \mathbf{A} , and shock variance d_c^j , and append the corresponding normal prior $\mathcal{N}(\tilde{\mathbf{m}}_c^j, d_c^j \tilde{\mathbf{M}}_c^j)$ as additional observations. To do this, let $\tilde{\mathbf{P}}_c^j$ be the Cholesky factor of $(\tilde{\mathbf{M}}_c^j)^{-1}$, i.e. $(\tilde{\mathbf{M}}_c^j)^{-1} = \tilde{\mathbf{P}}_c^j \tilde{\mathbf{P}}_c^{j'}$. The properly augmented data for country c and structural equation j are defined as:

$$\begin{aligned}
\tilde{\mathbf{Y}}_c^j &= \begin{bmatrix} \mathbf{a}_c^j \mathbf{Y}' & \tilde{\mathbf{m}}_c^j \tilde{\mathbf{P}}_c^j \end{bmatrix}' \\
&\text{size: } (T+\tilde{k}+1) \times 1 \\
\tilde{\mathbf{X}}_c^j &= \begin{pmatrix} [\mathbf{X} \quad \mathbf{U}_{gT}^j] \tilde{\mathbf{R}}_c^B' \\ \tilde{\mathbf{P}}_c^{j'} \end{pmatrix} \\
&\text{size: } (T+\tilde{k}+1) \times (\tilde{k}+1)
\end{aligned}$$

Conditional on global shocks \mathbf{U}_{gT} , these augmented data can be used to derive the

posterior distributions of $\mathbf{A}, \tilde{\mathbf{B}}, \chi, \mathbf{D}$ just as in [Baumeister and Hamilton \(2015\)](#):²

$$p(\mathbf{A} | \mathbf{Y}_T, \mathbf{U}_{gT}) \propto p(\mathbf{A}) [\det(\mathbf{A} \hat{\Omega} \mathbf{A}')]^{T/2} \prod_{c=1}^C \prod_{j=1}^J \frac{\left| \tilde{\mathbf{M}}_c^{j*} \right|^{1/2}}{\left| \tilde{\mathbf{M}}_c^j \right|^{1/2}} \frac{(\tau_c^j)^{\kappa_c^j}}{(2\tau_c^{j*}/T)^{\kappa_c^{j*}}} \frac{\Gamma((\kappa_c^j)^*)}{\Gamma(\kappa_c^j)} \quad (\text{C.4})$$

$$p(\mathbf{D} | \mathbf{A}, \mathbf{Y}_T, \mathbf{U}_{gT}) = \prod_{c=1}^C \prod_{j=1}^J \gamma \left((d_c^j)^{-1}; \kappa_c^{j*}, \tau_c^{j*} \right) \quad (\text{C.5})$$

$$p \left(\left(\tilde{\mathbf{B}}, \chi \right) | \mathbf{A}, \mathbf{D}, \mathbf{Y}_T, \mathbf{U}_{gT} \right) = \prod_{c=1}^C \prod_{j=1}^J \phi \left(\left(\tilde{\mathbf{b}}_c^j, \chi_c^j \right); \tilde{\mathbf{m}}_c^{j*}, \tilde{\mathbf{M}}_c^{j*} \right) \quad (\text{C.6})$$

with

$$\begin{aligned} \kappa_c^{j*} &= \kappa_c^j + T/2 \\ \tau_c^{j*} &= \tau_c^j + \zeta_c^{j*}/2 \\ \zeta_c^{j*} &= \tilde{\mathbf{Y}}_c^{j'} \tilde{\mathbf{Y}}_c^j - \tilde{\mathbf{Y}}_c^{j'} \tilde{\mathbf{X}}_c^j \left(\tilde{\mathbf{X}}_c^{j'} \tilde{\mathbf{X}}_c^j \right)^{-1} \tilde{\mathbf{X}}_c^{j'} \tilde{\mathbf{Y}}_c^j \\ \tilde{\mathbf{m}}_c^{j*} &= \left[\left(\tilde{\mathbf{X}}_c^{j'} \tilde{\mathbf{X}}_c^j \right)^{-1} \tilde{\mathbf{X}}_c^{j'} \tilde{\mathbf{Y}}_c^j \right]' \\ \tilde{\mathbf{M}}_c^{j*} &= \left(\tilde{\mathbf{X}}_c^{j'} \tilde{\mathbf{X}}_c^j \right)^{-1}. \end{aligned}$$

For equations without a global shock, the model simplifies further, as the additional column for the global shock \mathbf{U}_{gT}^j is dropped from $\tilde{\mathbf{X}}_c^j$. In this case, the corresponding equations in [C.6](#) describe multivariate distributions on lag coefficients, but no loading ($\phi \left(\tilde{\mathbf{b}}_c^j; \tilde{\mathbf{m}}_c^{j*}, \tilde{\mathbf{M}}_c^{j*} \right)$).

In order to derive the conditional posterior distribution for global shocks \mathbf{U}_{gT} , we first note that data and global shocks $(\mathbf{Y}_t, \mathbf{u}_{gt})$ are jointly normally distributed ([Geweke and Zhou, 1996](#)):

$$\begin{bmatrix} \mathbf{u}_{gt} \\ \mathbf{Y}_t \end{bmatrix} \sim \mathcal{N} \left(\begin{bmatrix} \mathbf{0} \\ \mathbf{A}^{-1} \mathbf{B} \mathbf{X}_{t-1} \end{bmatrix}, \begin{bmatrix} \mathbf{I}_G & (\chi \mathbf{A}^{-1})' \\ \mathbf{A}^{-1} \chi & \mathbf{A}^{-1} (\chi \chi' + \mathbf{D}) (\mathbf{A}^{-1})' \end{bmatrix} \right), \quad t \in \{1, \dots, T\}$$

We use this to derive the posterior distribution of global shocks, conditional on the data

²In [Baumeister and Hamilton \(2015, 2018\)](#), only the Cholesky factor $\tilde{\mathbf{P}}_c^j$ varies by equation. In our case, this also applies to the data observations due to the country-specific homogeneity restrictions and the equation-specific global shocks. However, this is not a concern as long as we can estimate $\tilde{\mathbf{B}}$ and χ equation-by-equation, i.e., as long as structural domestic shocks are mutually independent.

and all structural coefficients and loadings:

$$p(\mathbf{u}_{gt}|\tilde{\mathbf{B}}, \chi, \mathbf{A}, \mathbf{D}, \mathbf{Y}_t) \sim \phi(\mathbf{u}_{gt}; \mathbf{m}_{gt}^*, \mathbf{M}_g^*), \quad t \in \{1, \dots, T\} \quad (\text{C.7})$$

$$\mathbf{m}_{gt}^* = \chi' \left(\chi \chi' + \mathbf{D} \right)^{-1} (\mathbf{A} \mathbf{Y}_t - \mathbf{B} \mathbf{X}_{t-1}) \quad (\text{C.8})$$

$$\mathbf{M}_g^* = \mathbf{I} - \chi' \left(\chi \chi' + \mathbf{D} \right)^{-1} \chi, \quad t \in \{1, \dots, T\} \quad (\text{C.9})$$

We use a Metropolis-within-Gibbs to generate draws from the posterior distributions. As initial draws, we use the prior mean of \mathbf{A} , and random draws from a standard-normal distribution for \mathbf{U}_{gT} . Afterwards, every draw of $(\mathbf{A}, \mathbf{D}, \mathbf{B}, \chi, \mathbf{U}_{gT})$ is obtained from the following sequence:

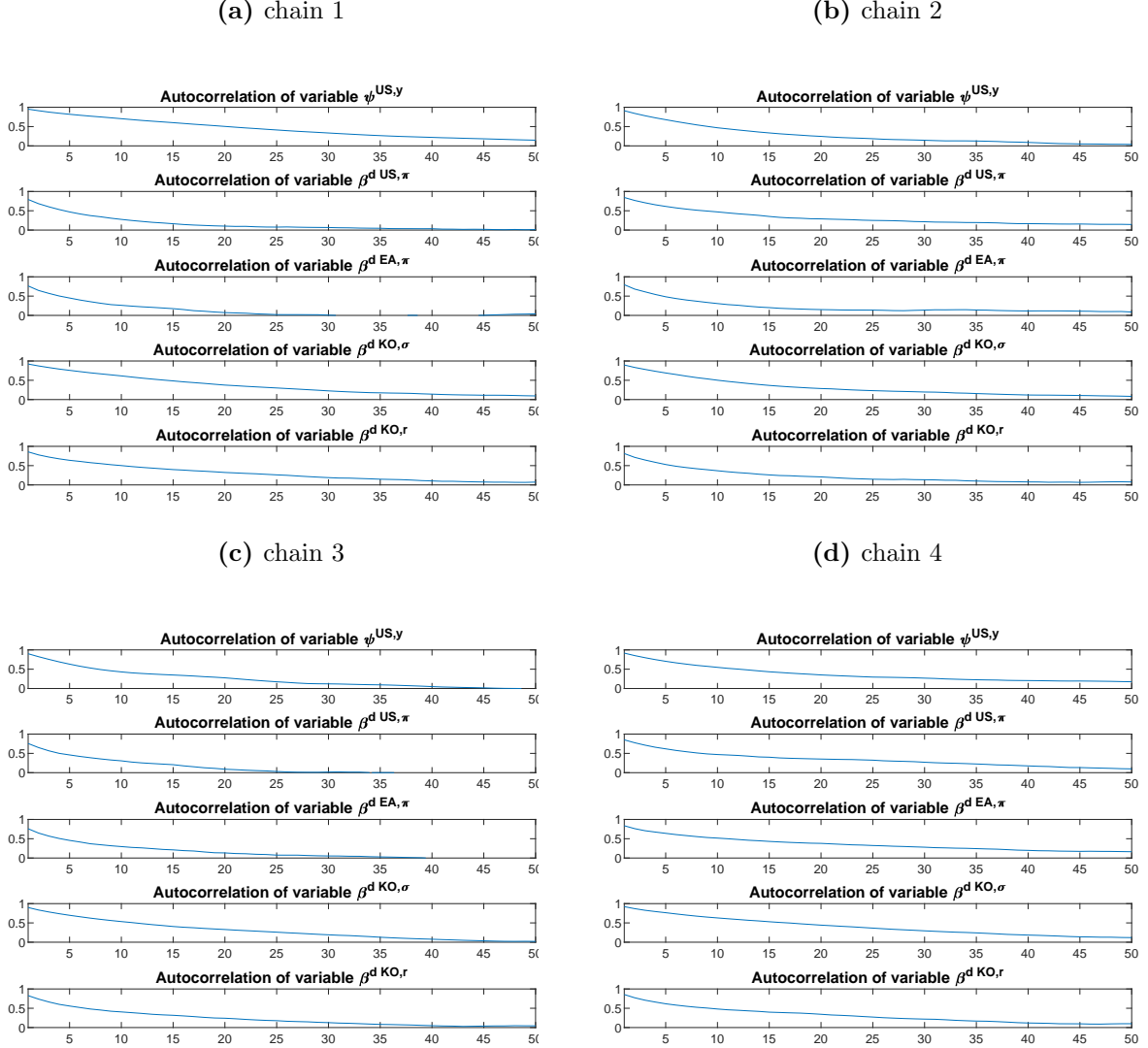
1. Draw \mathbf{A} from $p(\mathbf{A}|\mathbf{Y}_T, \mathbf{U}_{gT})$, equation (C.4), using a single Metropolis-Hastings step with parameters grouped in C random blocks.
2. For every country c and structural equation j , ...
 - (a) ... draw $(d_c^j)^{-1}$ from $p(\mathbf{D}|\mathbf{A}, \mathbf{Y}_T, \mathbf{U}_{gT})$, equation (C.5).
 - (b) ... draw $(\tilde{\mathbf{b}}_c^j, \chi_c^j)$ jointly from $p\left(\left(\tilde{\mathbf{B}}, \chi\right) | \mathbf{A}, \mathbf{D}, \mathbf{Y}_T, \mathbf{U}_{gT}\right)$, equation (C.6). No loadings are drawn for structural equations j without a corresponding global shock.
3. Draw \mathbf{U}_{gT} from $p(\mathbf{u}_{gt}|\tilde{\mathbf{B}}, \chi, \mathbf{A}, \mathbf{D}, \mathbf{Y}_t)$ for all observations t , equation (C.7).
4. Use homogeneity restrictions (C.2) to derive \mathbf{B} from restricted coefficients $\tilde{\mathbf{b}}_c^j$.

The original algorithm of [Baumeister and Hamilton \(2015\)](#) uses the mode of the prior likelihood as starting values and its Hessian to guide the most promising search directions for the Metropolis-Hastings steps. Due to the larger number of free parameters in \mathbf{A} (84 in our case), numerical likelihood maximization fails. Therefore, we use a pre-sampling with a single chain to obtain suitable starting values and search directions for draws of \mathbf{A} . We run the pre-sampling such that we obtain twice as many draws as the number of free parameters in \mathbf{A} after 400'000 burn-in and thinning of 500 draws (total chain length: 484'000 draws). The main algorithm runs on 4 parallel chains. From each chain, we obtain 450,000 draws and keep every 50th draw after a burn-in of 200,000 draws, for a total of 20'000 retained draws from the posterior distribution.

C.4 Convergence statistics

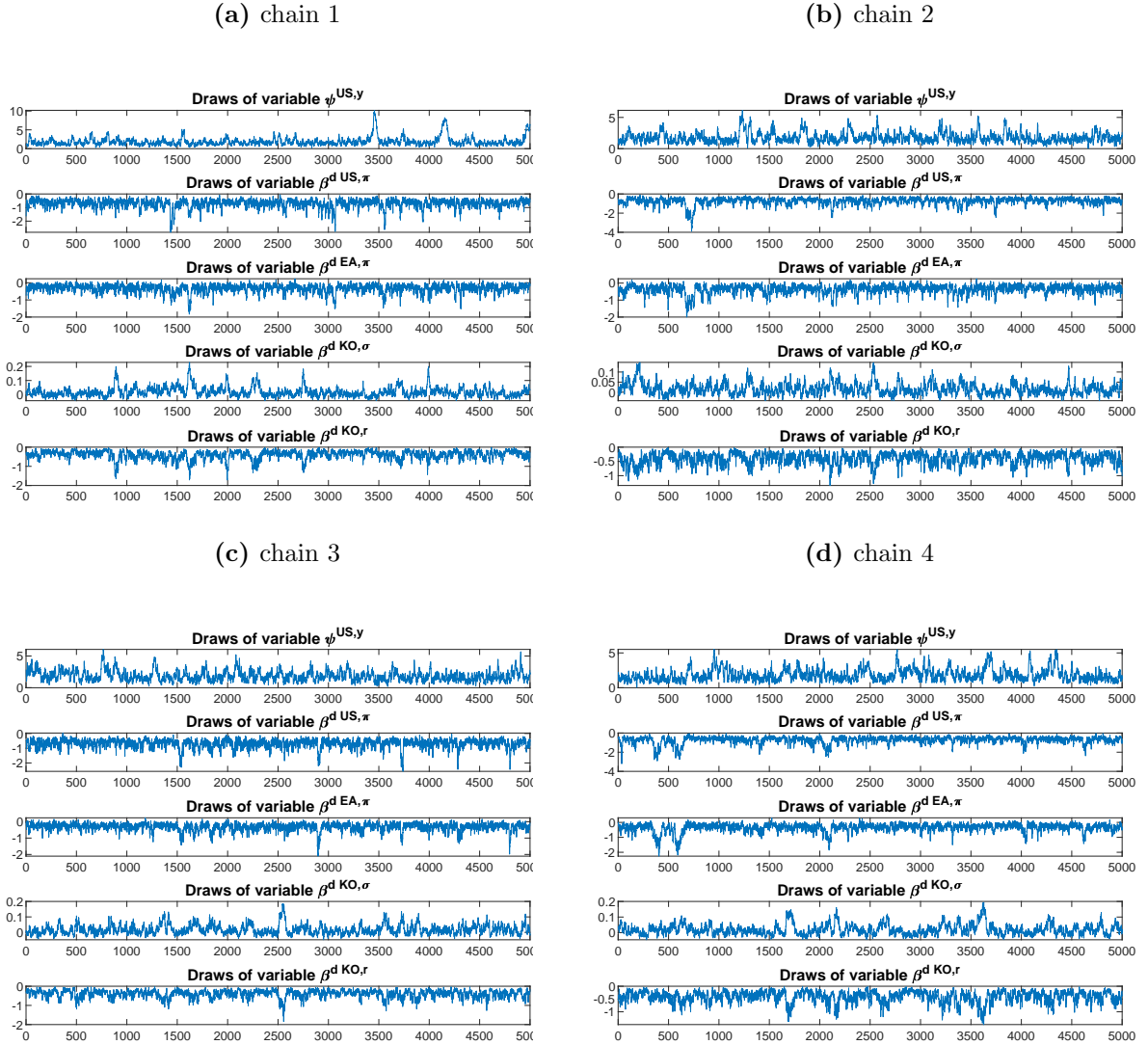
Figure C.1 and C.2 plots the autocorrelation across draws (after burn-in) and plots all draws for the four chains exemplary for the coefficients which have the weakest convergence statistics.

Figure C.1: Autocorrelations of draws



NOTES: The plots show the autocorrelation across draws (after burn-in) of the structural parameters with the weakest convergence statistics (per plot) exemplary for the four chains.

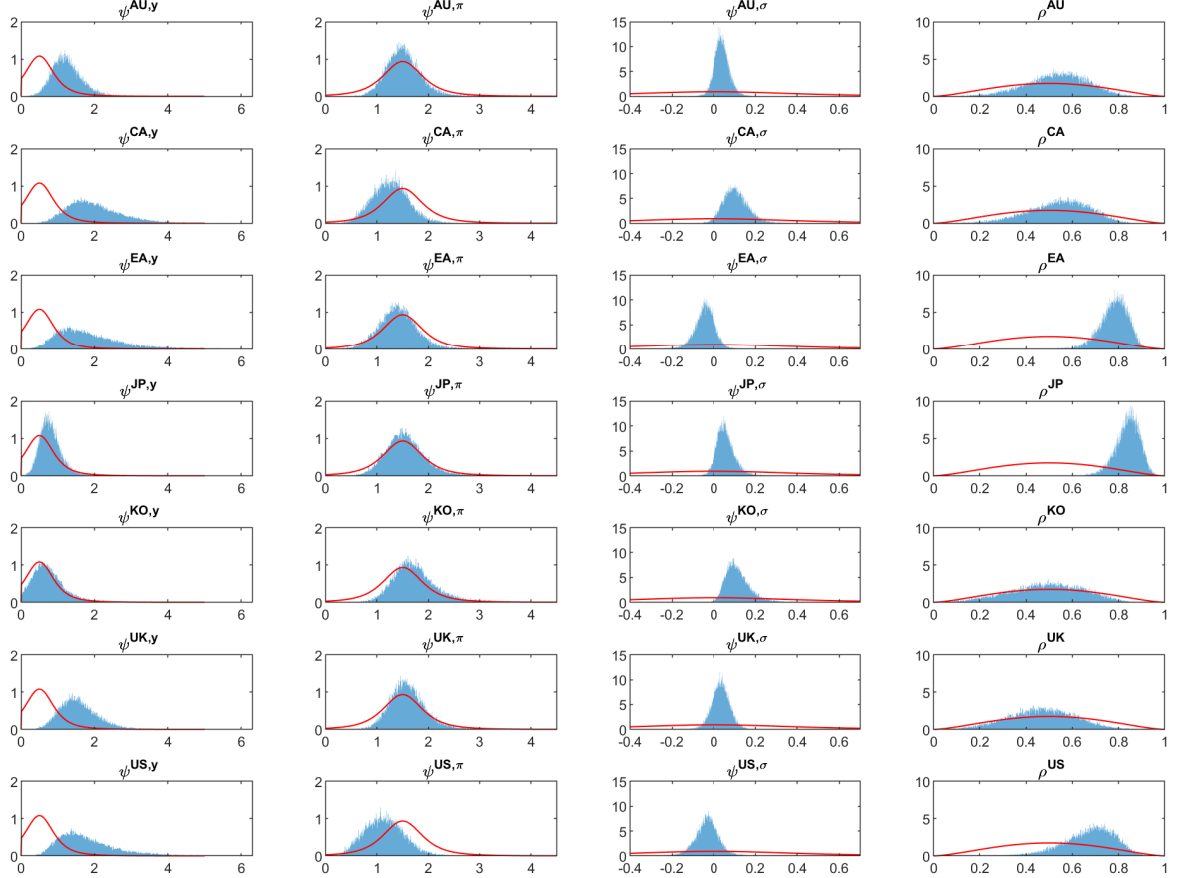
Figure C.2: Trace plot of draws



NOTES: Trace plots of the structural parameters with the weakest convergence statistics (per plot) exemplary for the four chains.

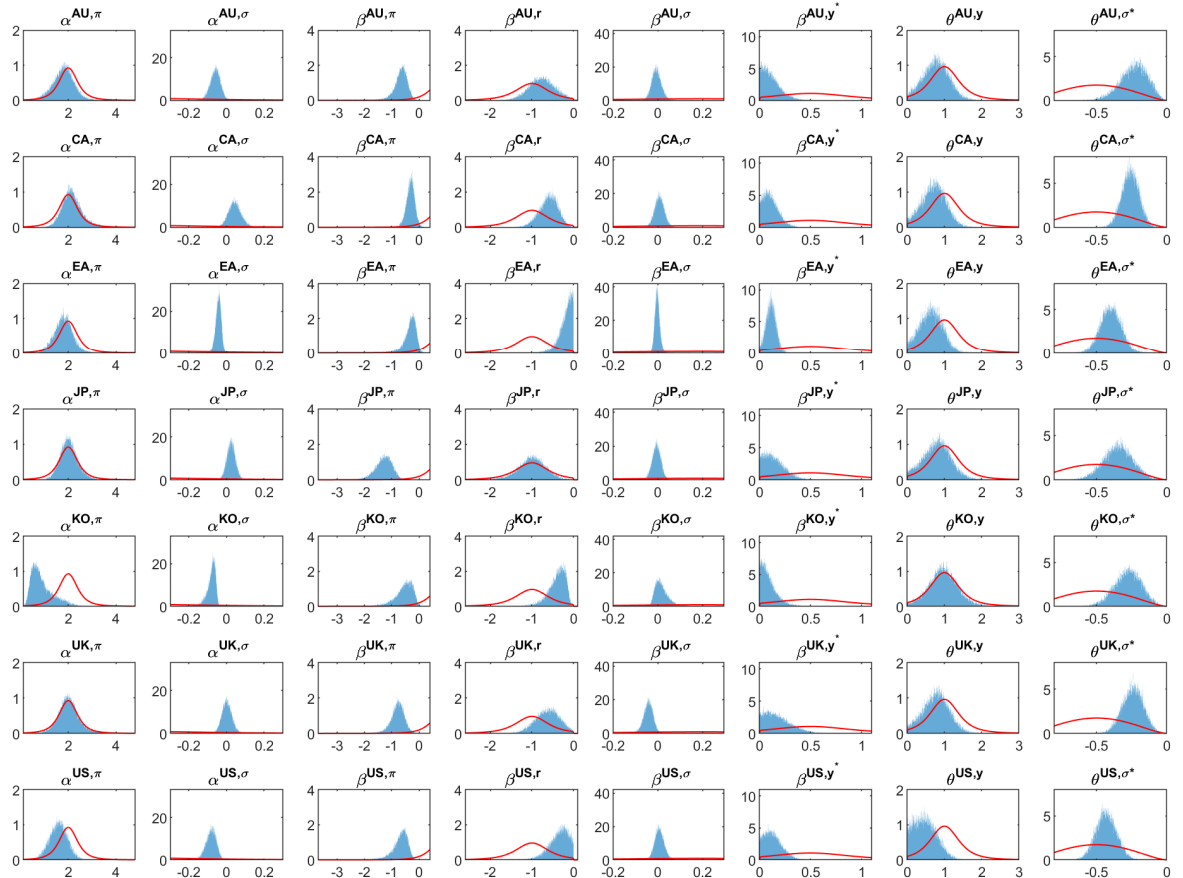
D Further results

Figure D.3: Structural contemporaneous parameters of the monetary policy rules



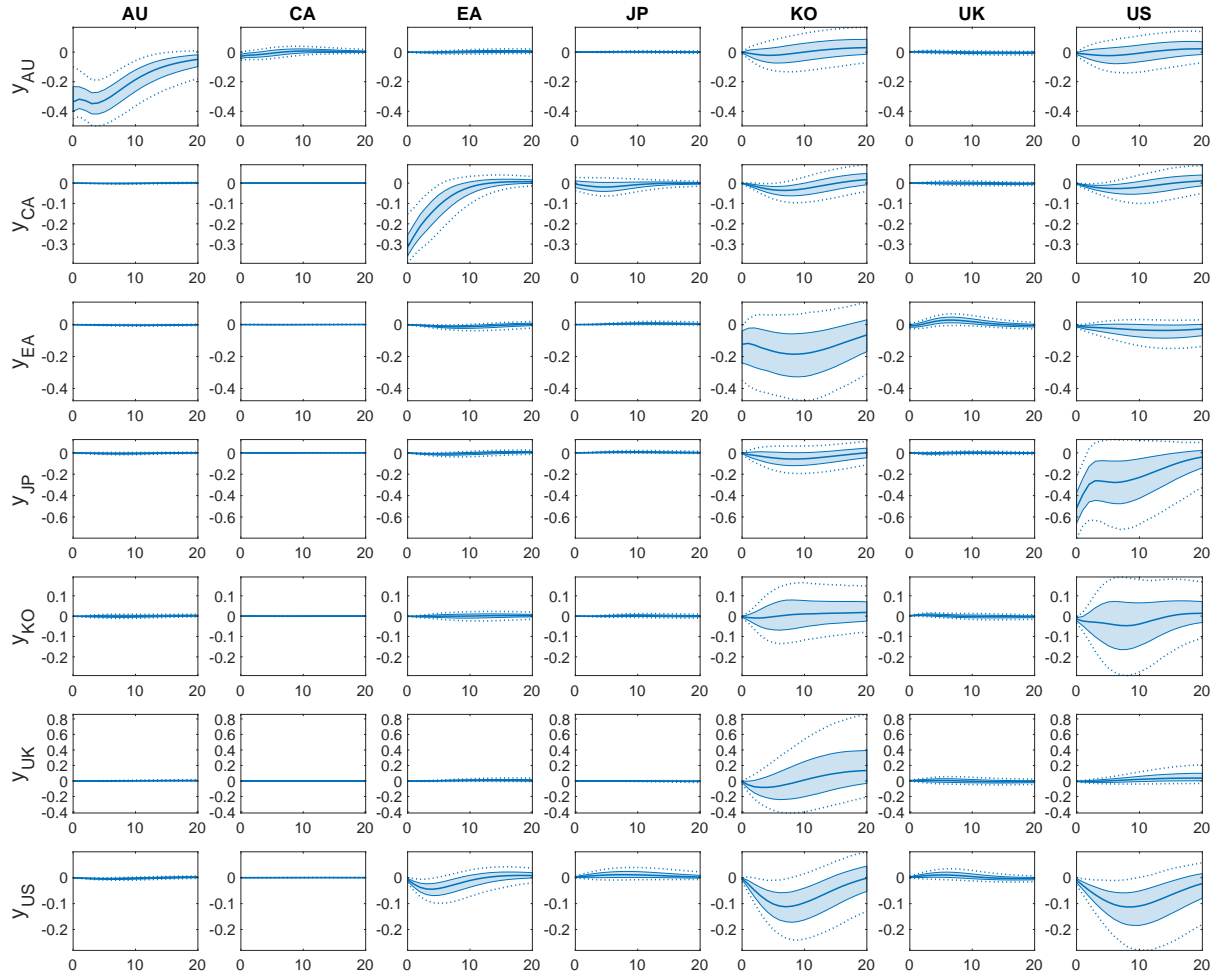
NOTES: The solid red lines in the figure show the prior distribution of the structural contemporaneous parameters (columns: parameters; rows: countries). The histograms show posterior distributions.

Figure D.4: Structural contemporaneous parameters of remaining equations



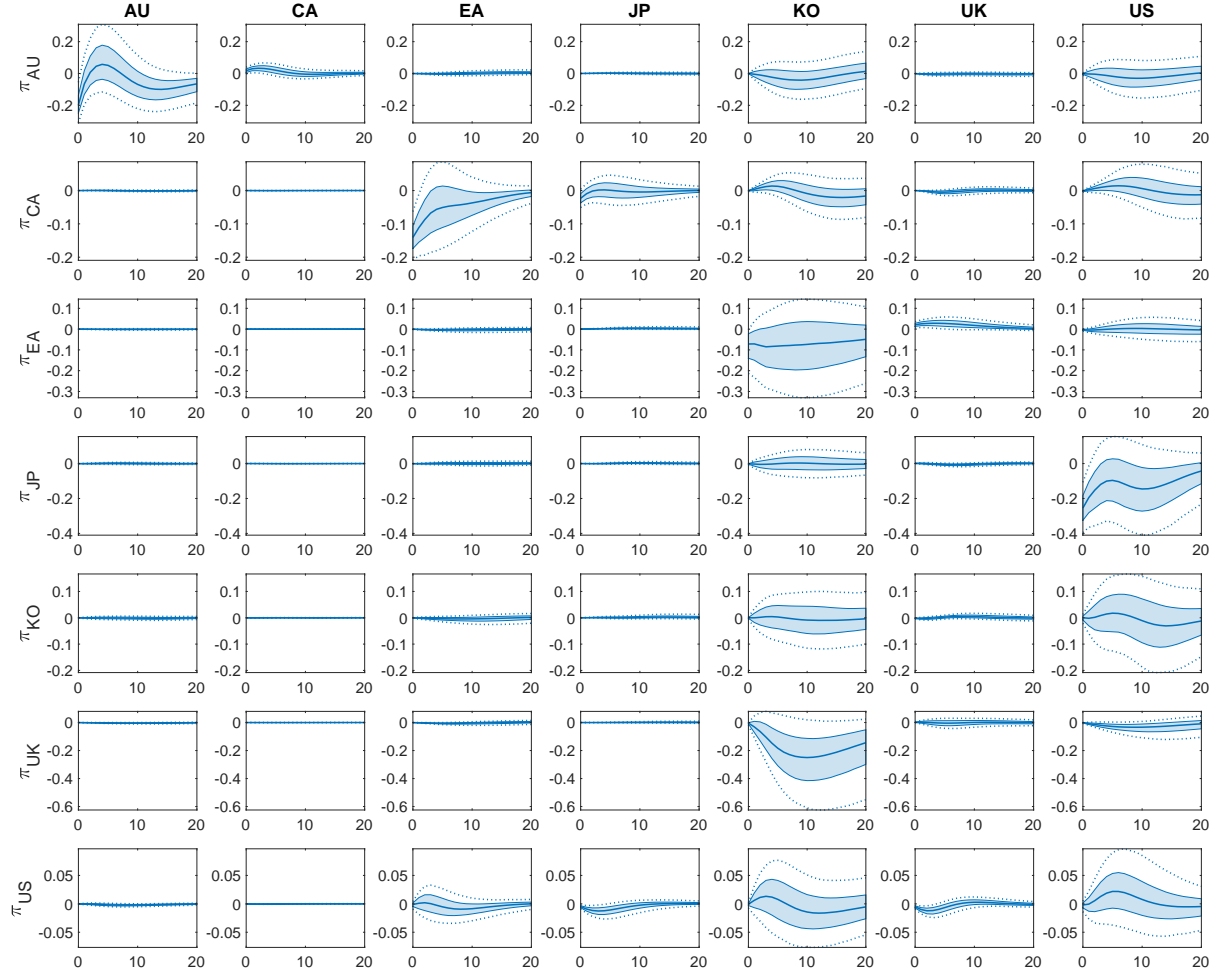
NOTES: The solid black lines in the figure show the prior distribution of the structural contemporaneous parameters. The histograms give the country-specific posterior distributions.

Figure D.5: Impulse responses of output gaps to country-specific monetary policy shocks



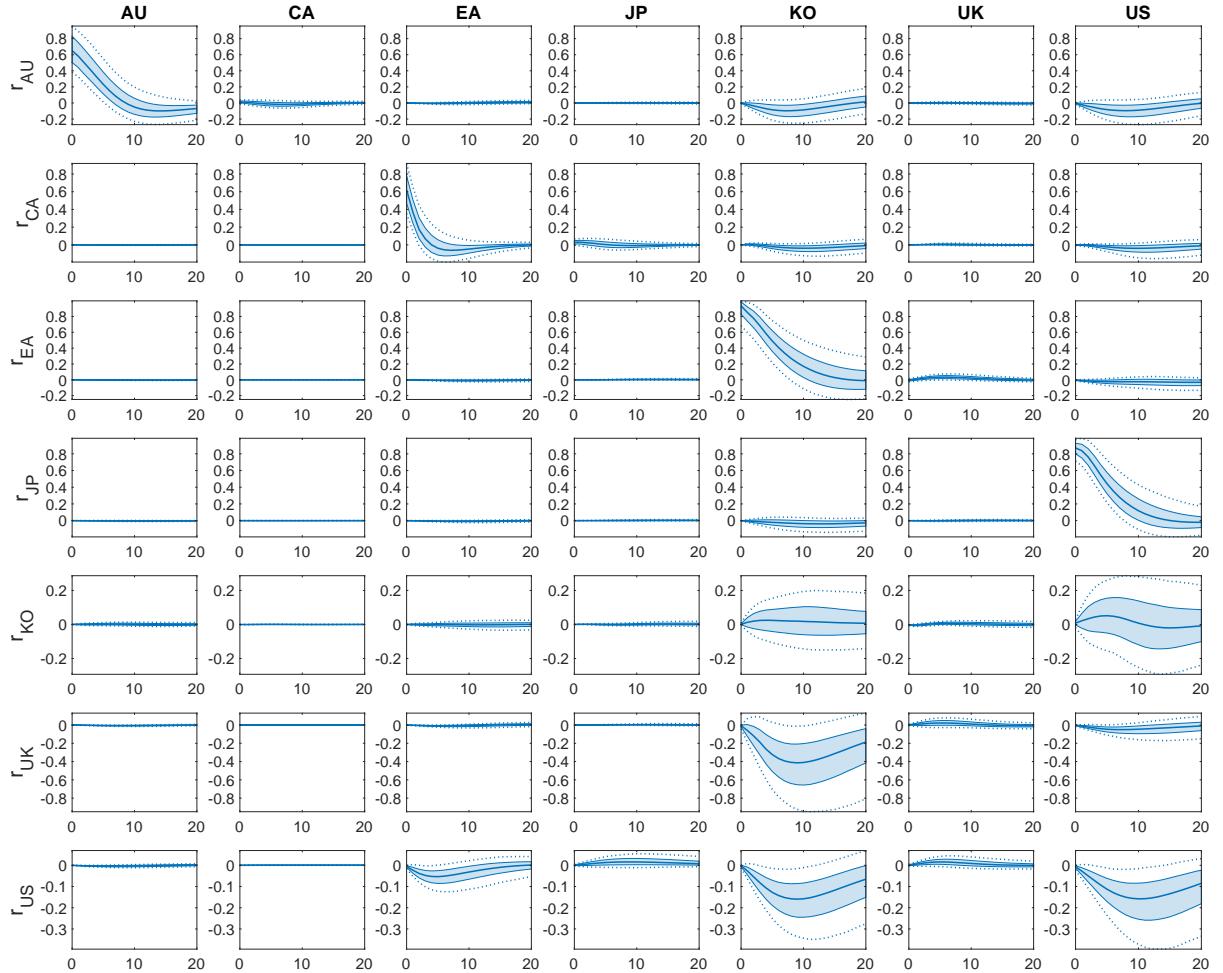
NOTES: The solid lines in the figure show median impulse responses of country-specific output gaps (in rows) to country-specific monetary shocks over 20 quarters. The shaded areas (dotted lines) show the 68% (95%) posterior credibility sets. The shocks have size of one unit.

Figure D.6: Impulse responses of inflation to country-specific monetary policy shocks



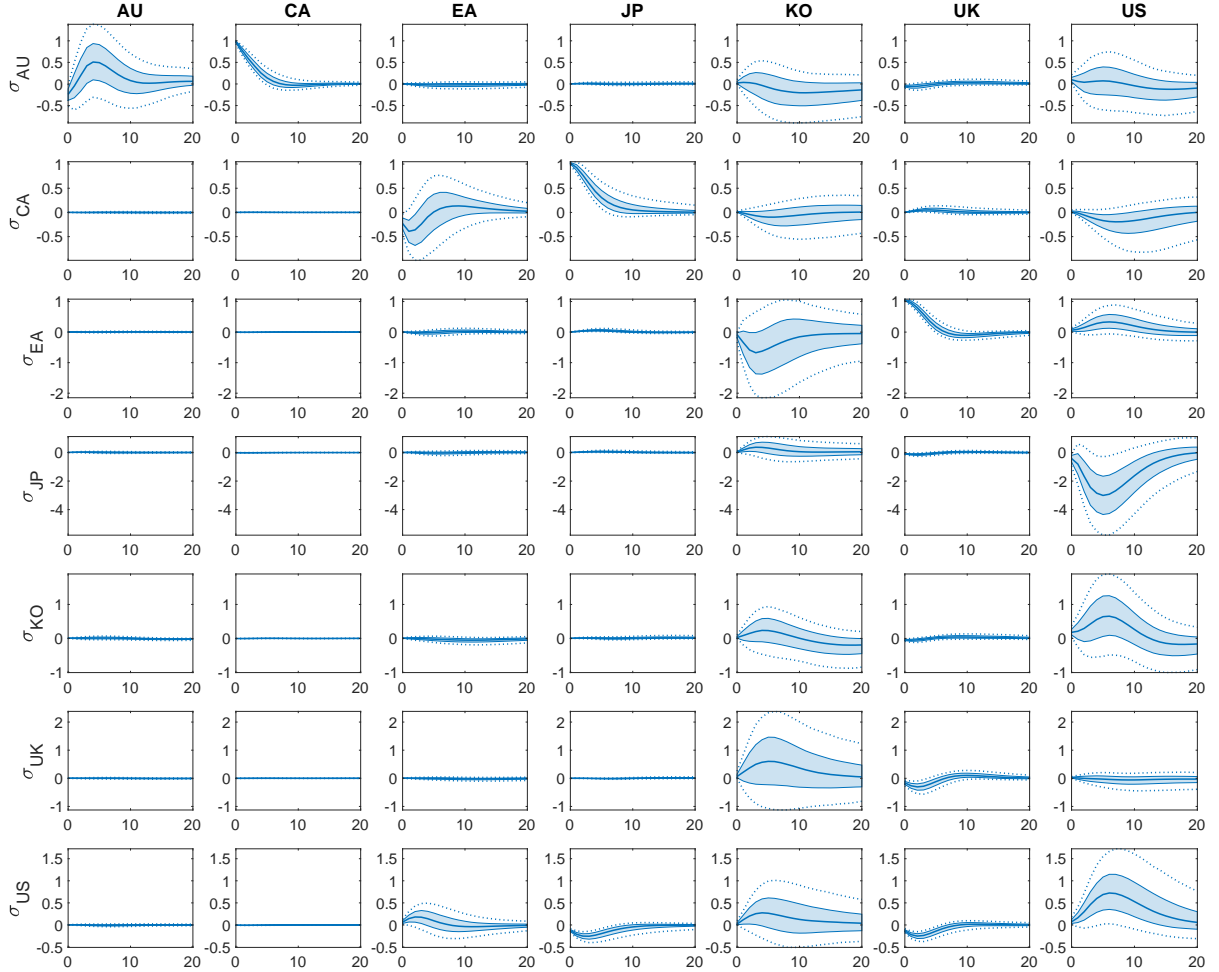
NOTES: The solid lines in the figure show median impulse responses of country-specific inflation (in rows) to country-specific monetary policy shocks over 20 quarters. The shaded areas (dotted lines) show the 68% (95%) posterior credibility sets. The shocks have size of one unit.

Figure D.7: Impulse responses of interest rates to country-specific monetary policy shocks



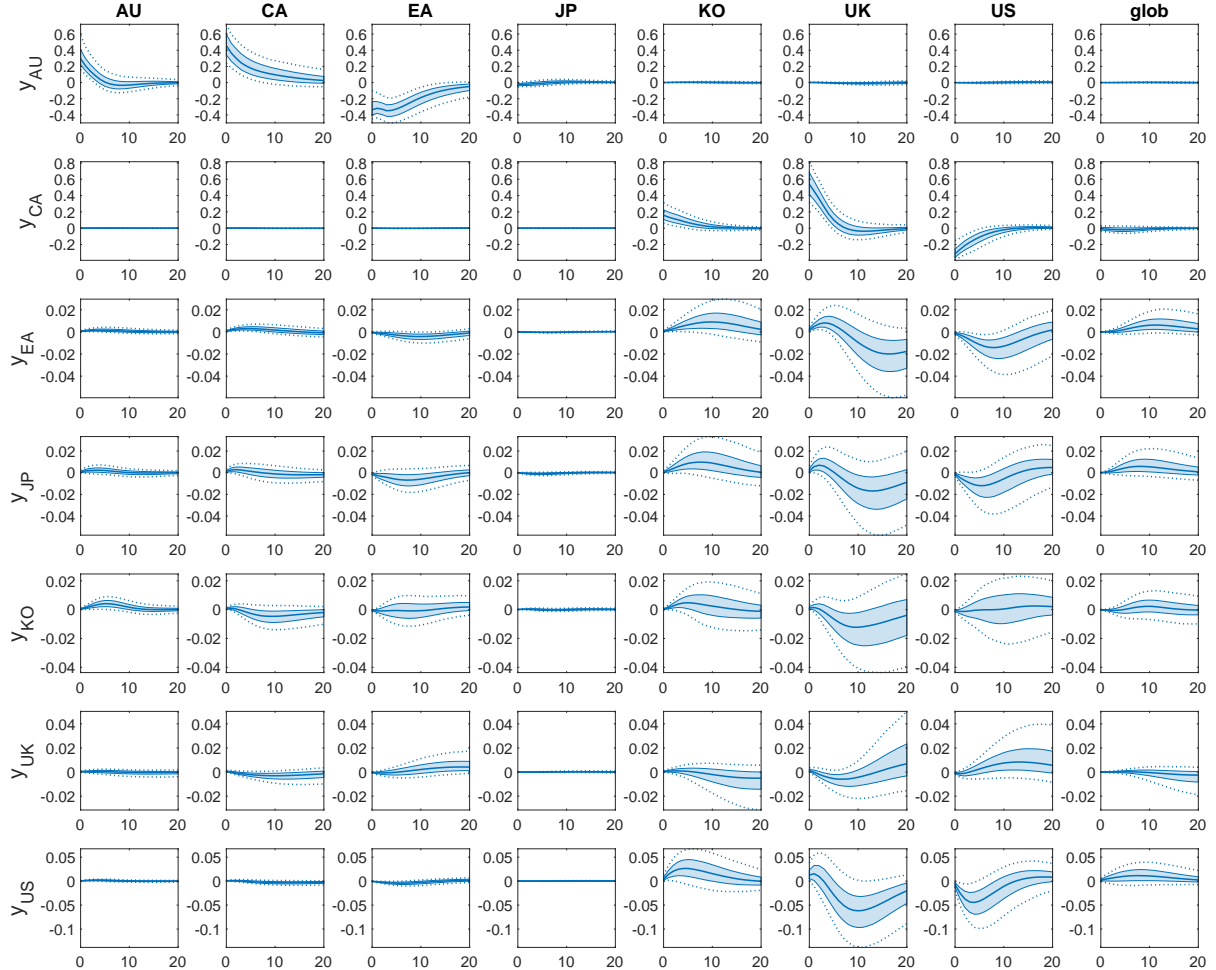
NOTES: The solid lines in the figure show median impulse responses of country-specific interest rates (in rows) to country-specific monetary policy shocks (in columns) over 20 quarters. The shaded areas (dotted lines) show the 68% (95%) posterior credibility sets. The shocks have size of one unit (i.e., one percentage point).

Figure D.8: Impulse responses of changes in exchange rates to country-specific monetary policy shocks



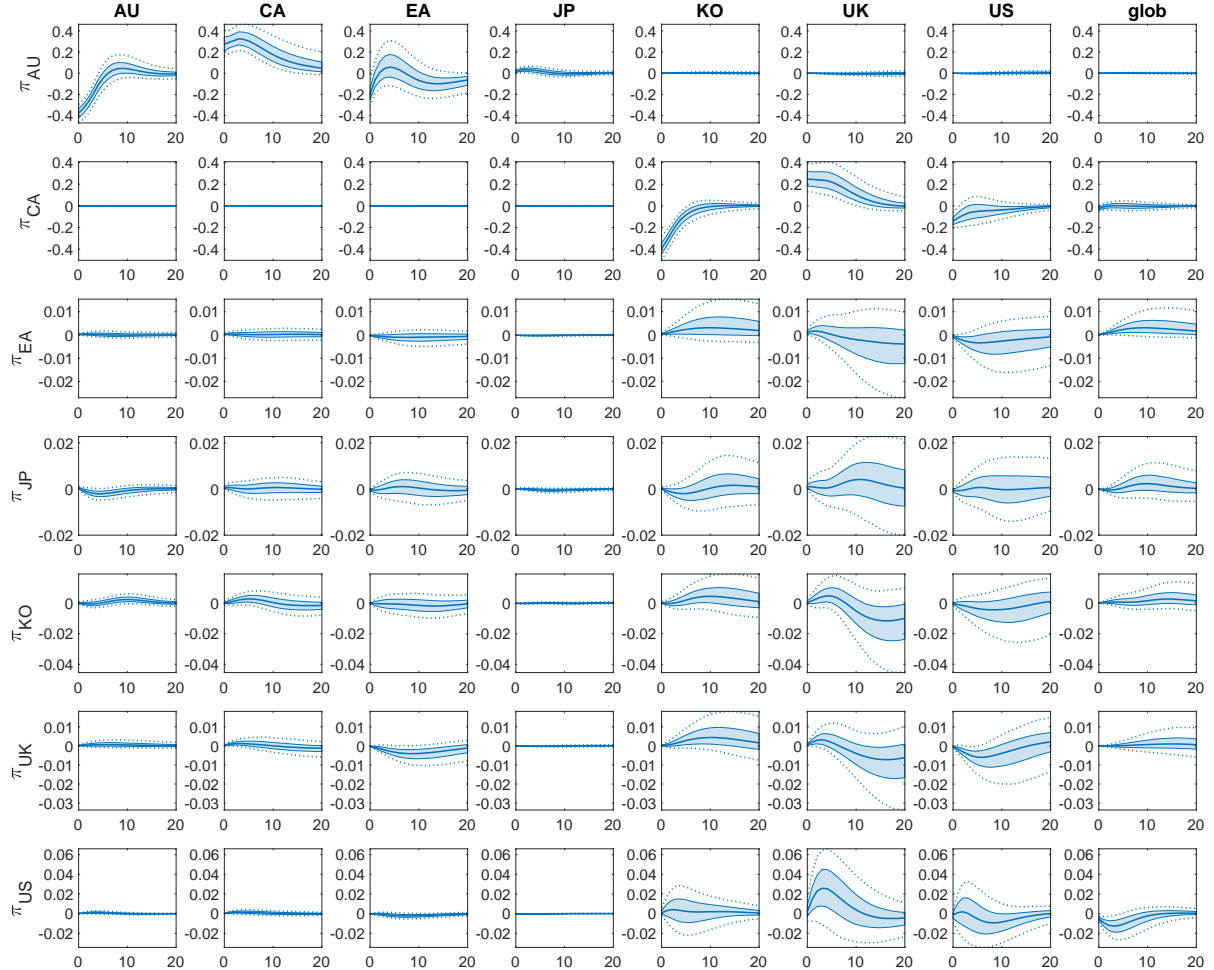
NOTES: The solid lines in the figure show median impulse responses of country-specific changes in exchange rates (in rows) to country-specific monetary policy shocks over 20 quarters. The shaded areas (dotted lines) show the 68% (95%) posterior credibility sets. The shocks have size of one unit.

Figure D.9: Impulse responses of output gaps to country-specific and global supply shocks



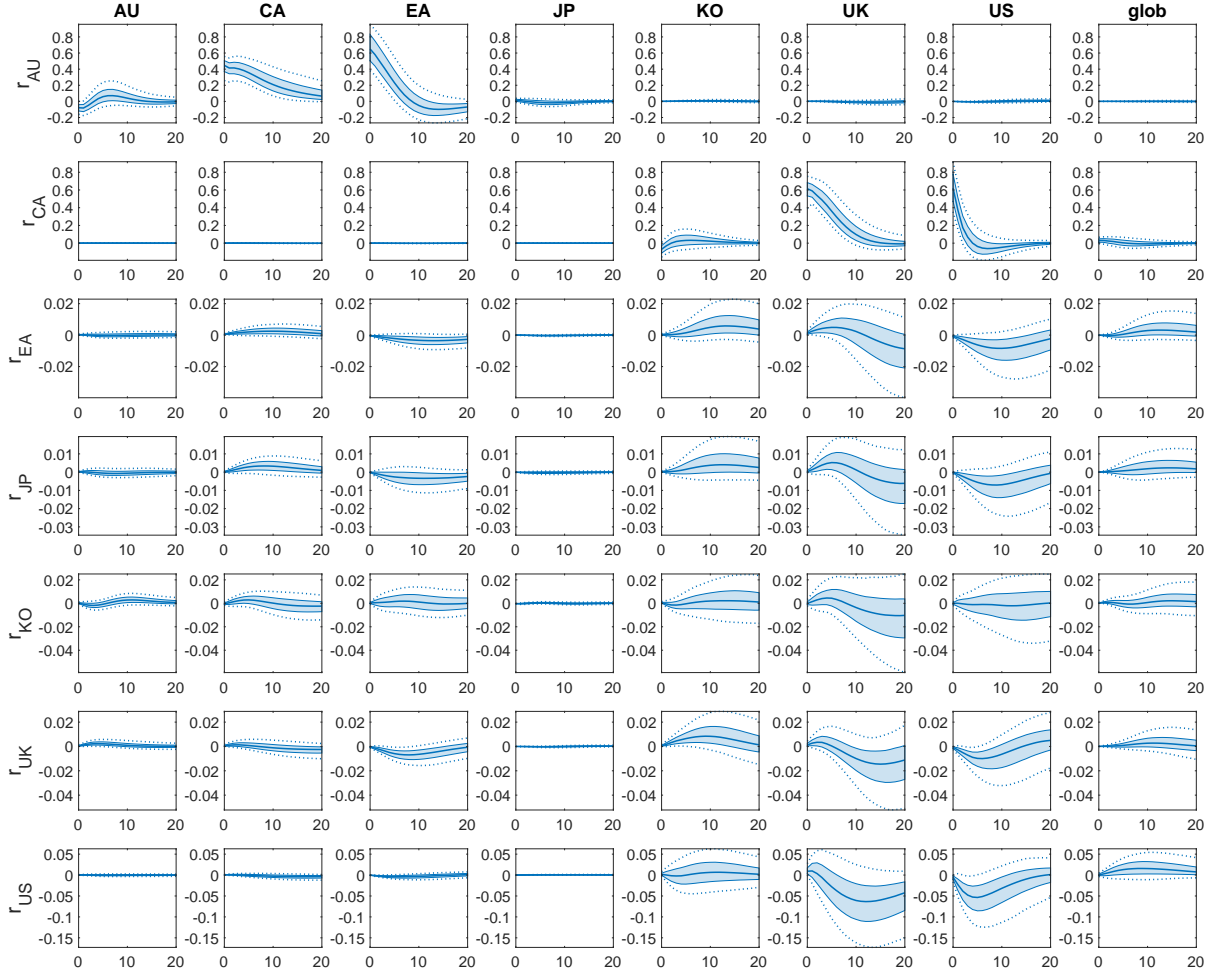
NOTES: The solid lines in the figure show median impulse responses of country-specific output gaps (in rows) to country-specific and global supply shocks over 20 quarters. The shaded areas (dotted lines) show the 68% (95%) posterior credibility sets. The shocks have size of one unit.

Figure D.10: Impulse responses of inflation to country-specific and global supply shocks



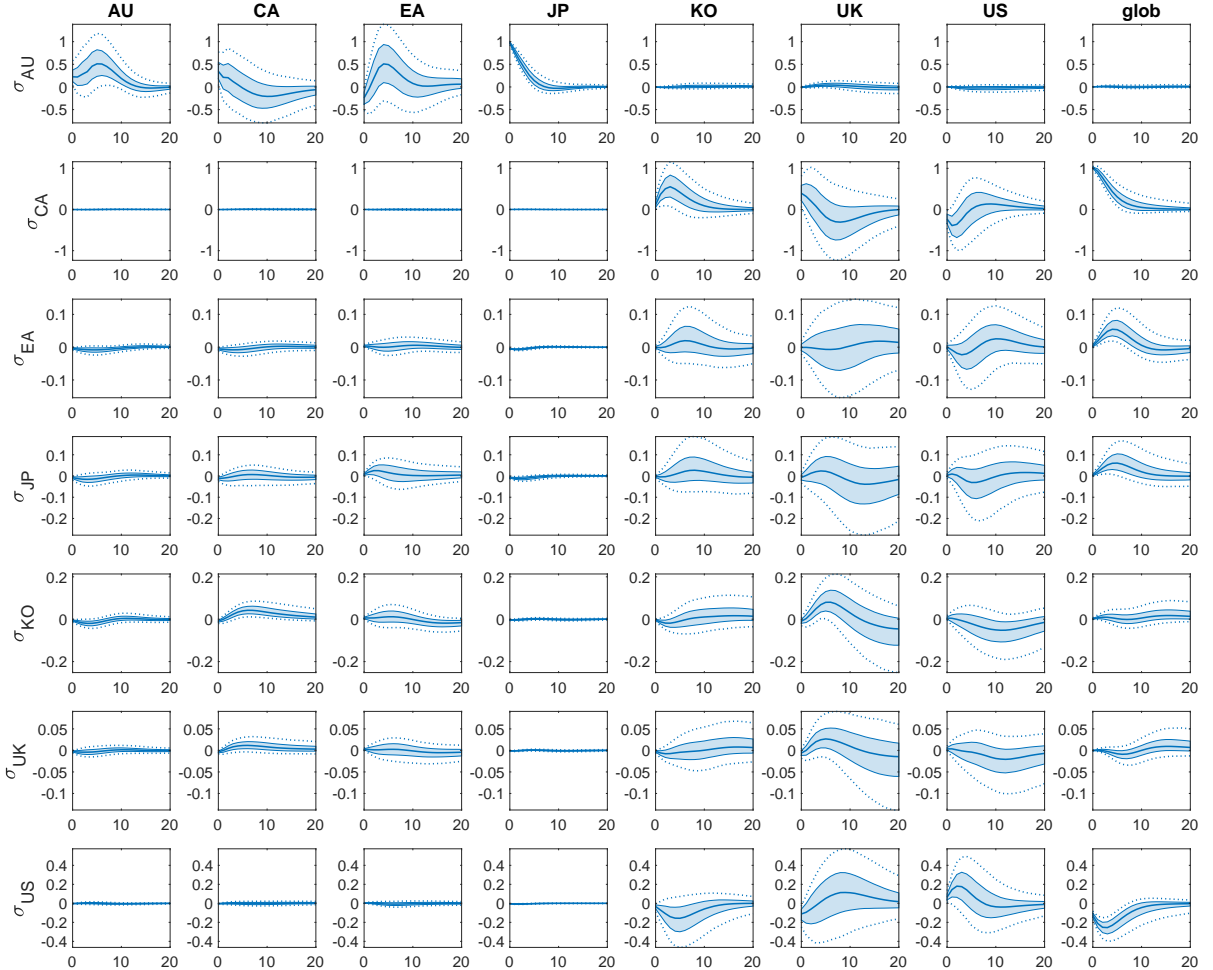
NOTES: The solid lines in the figure show median impulse responses of country-specific inflation (in rows) to country-specific and global supply shocks over 20 quarters. The shaded areas (dotted lines) show the 68% (95%) posterior credibility sets. The shocks have size of one unit.

Figure D.11: Impulse responses of interest rates to country-specific and global supply shocks



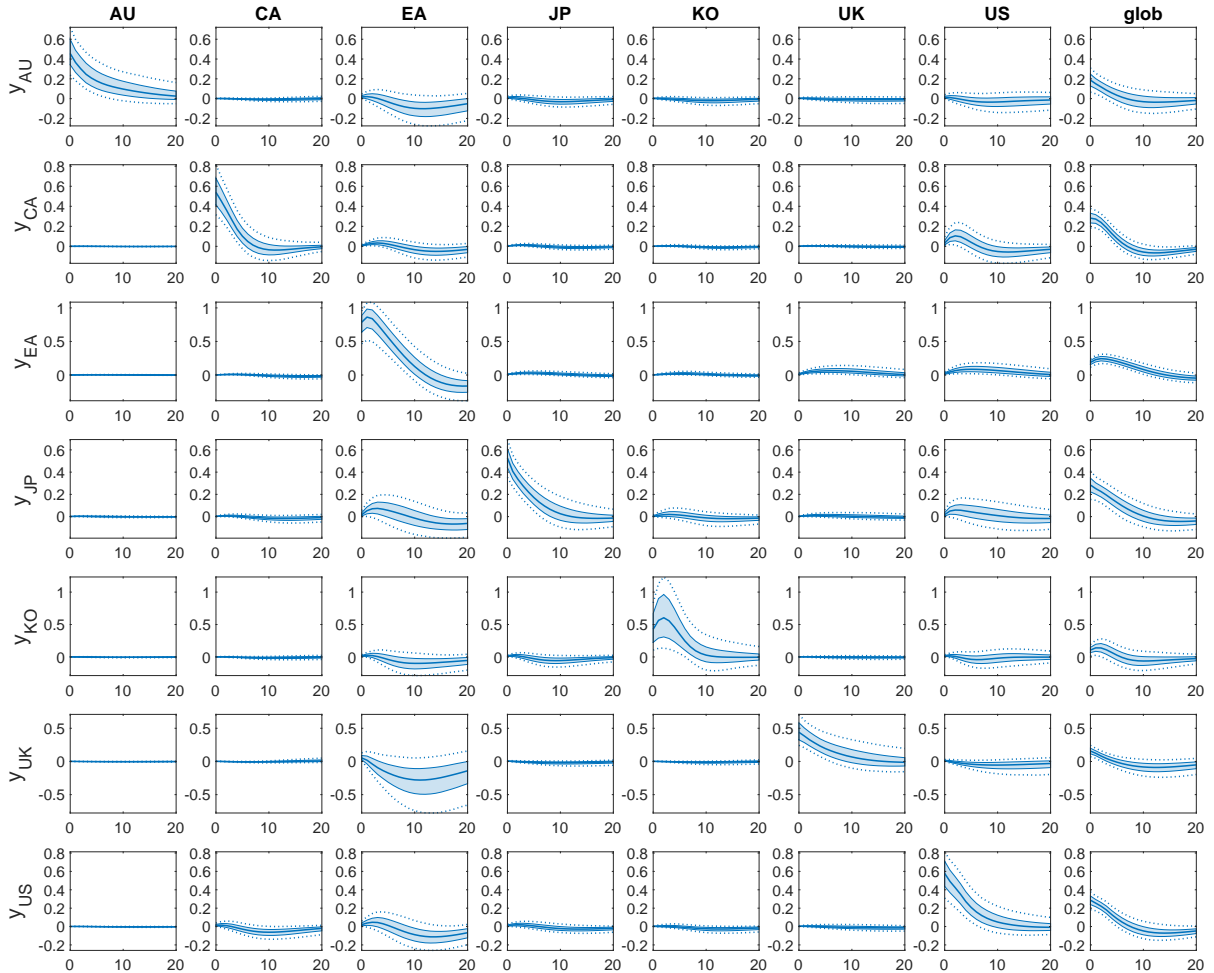
NOTES: The solid lines in the figure show median impulse responses of country-specific interest rates (in rows) to country-specific and global supply shocks over 20 quarters. The shaded areas (dotted lines) show the 68% (95%) posterior credibility sets. The shocks have size of one unit.

Figure D.12: Impulse responses of changes in exchange rates to country-specific and global supply shocks



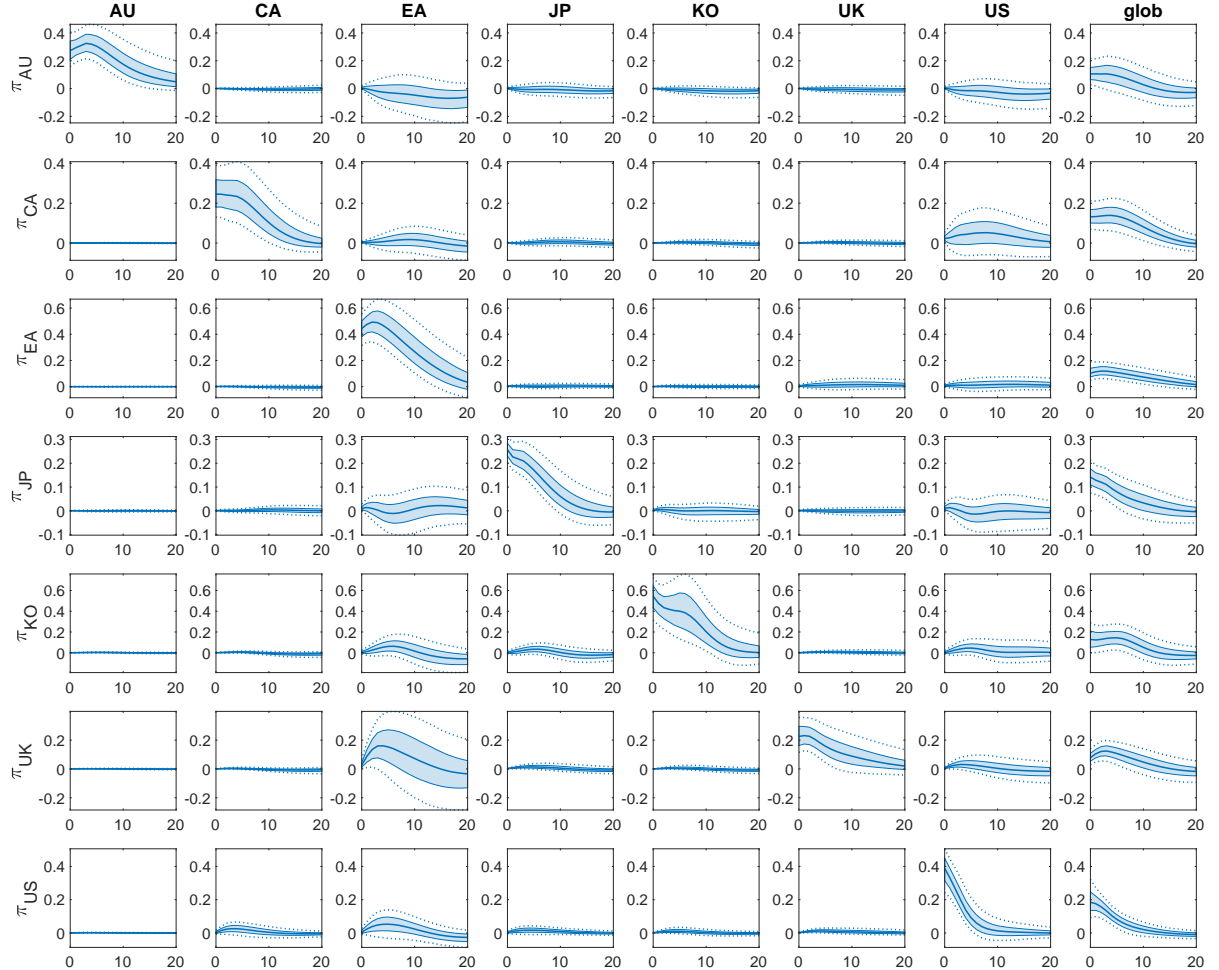
NOTES: The solid lines in the figure show median impulse responses of country-specific changes in exchange rates (in rows) to country-specific and global supply shocks over 20 quarters. The shaded areas (dotted lines) show the 68% (95%) posterior credibility sets. The shocks have size of one unit.

Figure D.13: Impulse responses of output gaps to country-specific and global demand shocks



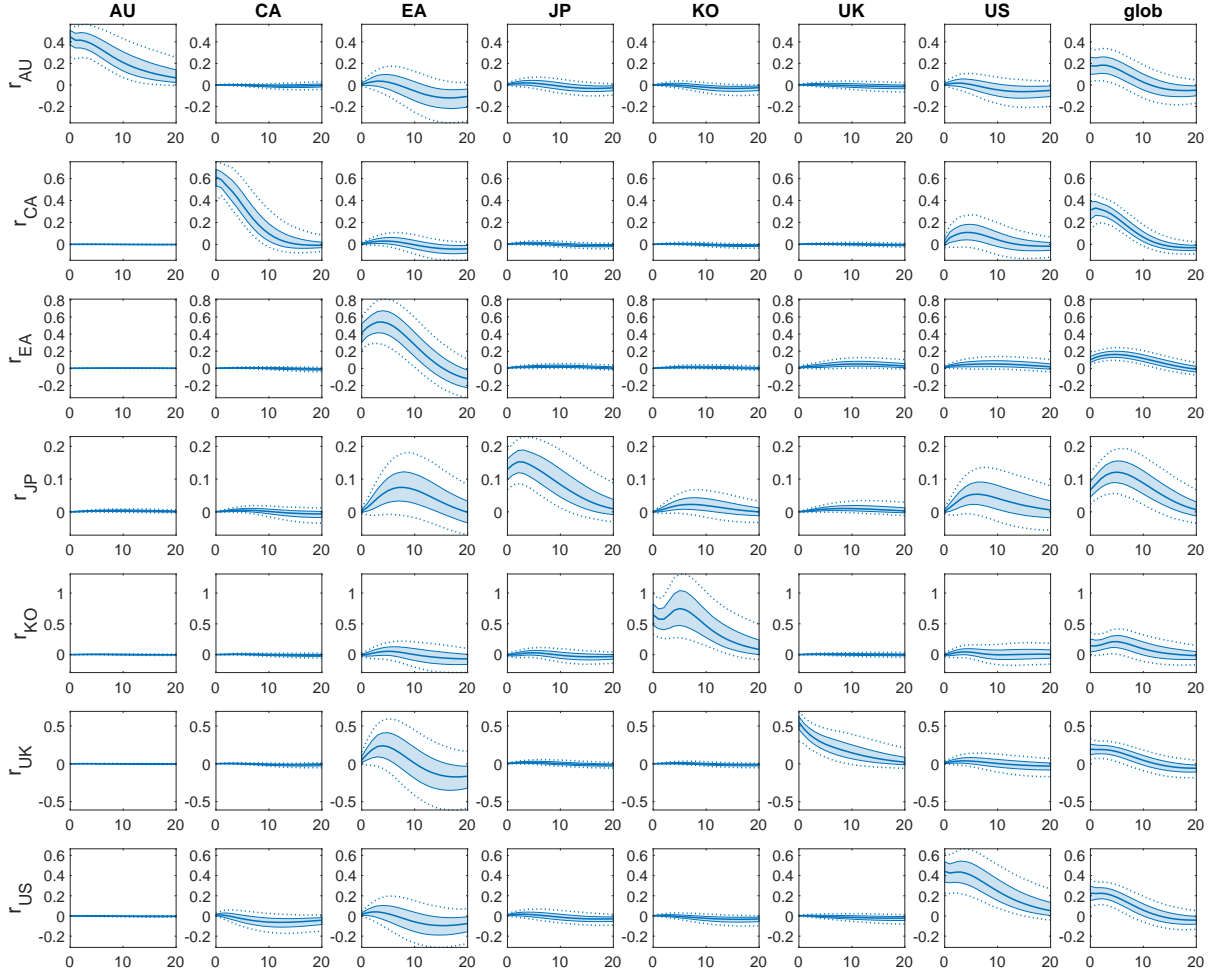
NOTES: The solid lines in the figure show median impulse responses of country-specific output gaps (in rows) to country-specific and global demand shocks over 20 quarters. The shaded areas (dotted lines) show the 68% (95%) posterior credibility sets. The shocks have size of one unit.

Figure D.14: Impulse responses of inflation to country-specific and global demand shocks



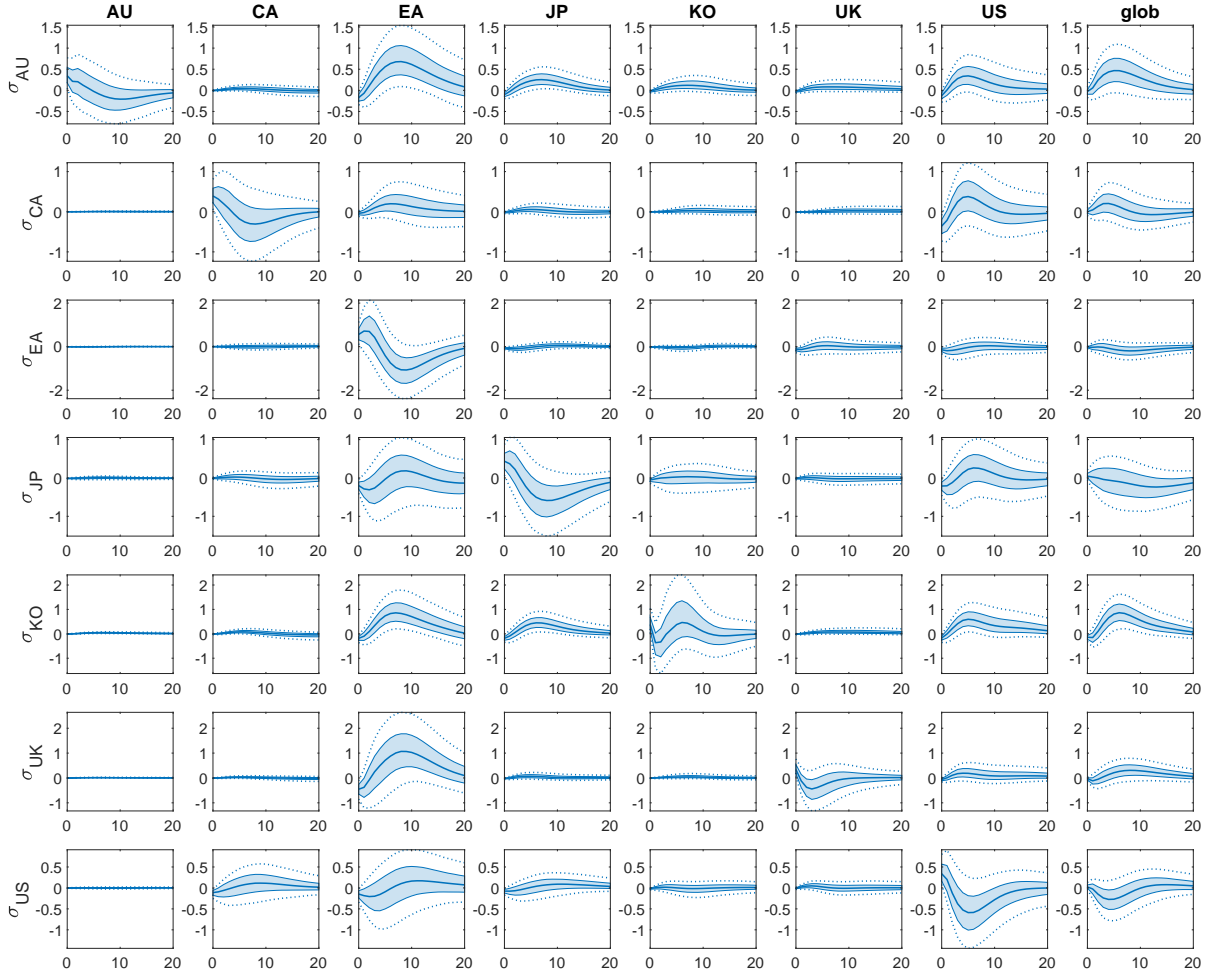
NOTES: The solid lines in the figure show median impulse responses of country-specific inflation (in rows) to country-specific and global demand shocks over 20 quarters. The shaded areas (dotted lines) show the 68% (95%) posterior credibility sets. The shocks have size of one unit.

Figure D.15: Impulse responses of interest rates to country-specific and global demand shocks



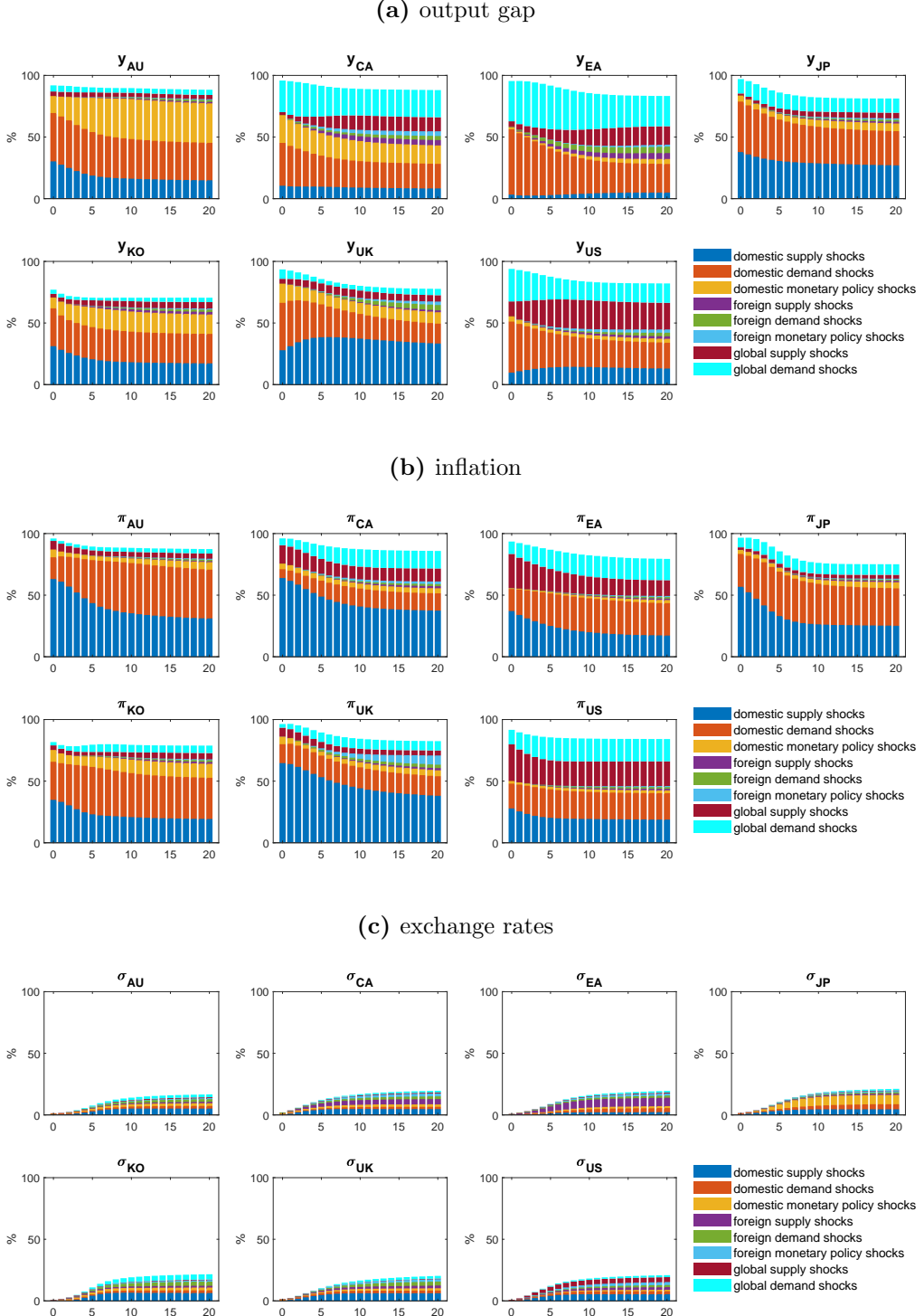
NOTES: The solid lines in the figure show median impulse responses of country-specific interest rates (in rows) to country-specific and global demand shocks over 20 quarters. The shaded areas (dotted lines) show the 68% (95%) posterior credibility sets. The shocks have size of one unit.

Figure D.16: Impulse responses of changes in exchange rates to country-specific and global demand shocks



NOTES: The solid lines in the figure show median impulse responses of country-specific changes in exchange rates (in rows) to country-specific and global demand shocks over 20 quarters. The shaded areas (dotted lines) show the 68% (95%) posterior credibility sets. The shocks have size of one unit.

Figure D.17: Forecast error variance decomposition of output gap, inflation and changes in exchange rates



NOTES: The figure shows the forecast error variance decomposition of country-specific output gap, inflation and changes in exchange rates (in subplots) to domestic, foreign and global shocks over 20 quarters. Foreign shocks are grouped for convenience of presentation. Unlabeled shares are explained by the residual shock to the exchange rate equation.

E Further robustness analysis

This sections shows results for several robustness checks changing the model set-up, using alternative weights, and adjusting the structural contemporaneous relations. In nearly all cases, we only show the forecast error variance decomposition of interest rates (Figures E.18 to E.36) and structural contemporaneous coefficients β^{c,y^*} (Figures E.37 to E.55) as a comparison to our main results. Further results are available on request.

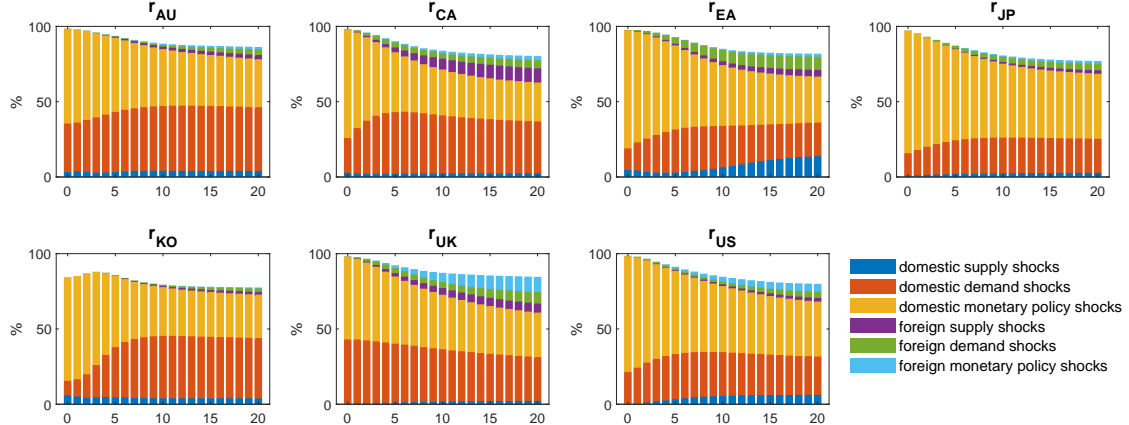
The alternative model specifications changing the model-set up are: a model without global shocks, a model with four global shocks, baseline model excluding a deterministic trend, baseline model with 8 lags, baseline model with data starting in 1990:Q1, baseline model with data ending in 2007:Q2.

Three specifications use alternative banking weights for foreign interest rates while the remaining foreign variables are trade-weighted: weights based on BIS data using total liabilities of the locational banking statistics (*LBS liabilities*), total claims of the locational banking statistics (*LBS claims*), and the consolidated banking statistics (*CBS*). The locational banking statistics include outstanding claims and liabilities of worldwide operating banks located in a reporting country. The consolidated banking statistics measure claims of banking groups whose headquarter are located in the reporting country.

Five specifications adjust the structural contemporaneous relations in the baseline in the following way: extends the monetary policy rules to contain coefficients on foreign interest rates, extends the monetary policy rules to contain coefficients on foreign inflation, extends the monetary policy rules to contain coefficients on foreign output gaps and foreign inflation, adds foreign output gaps in the supply equation, restricting the coefficient to be positive, adjusts the exchange rate equation such that interest rate differential enter.

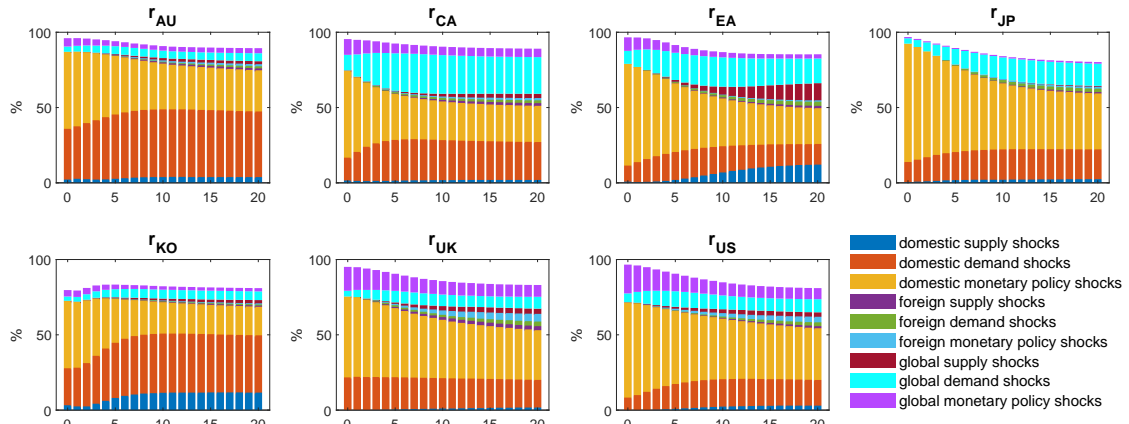
The remaining specifications add an additional channel variable to the baseline model: stock prices, term spreads, trade, exports or imports. Figures E.56 to E.60 show the impulse response functions of the channel variables to country-specific monetary policy shocks.

Figure E.18: Forecast error variance decomposition of interest rates - model without global shocks



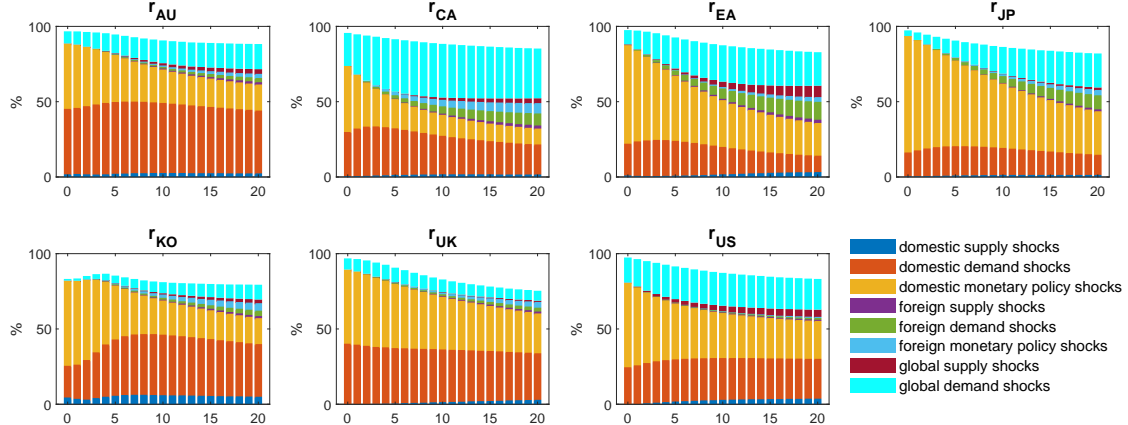
NOTES: The figure shows the forecast error variance decomposition of country-specific interest rates to domestic and foreign shocks over 20 quarters for the alternative model specification. Unlabeled shares are explained by the residual shock to the exchange rate equation.

Figure E.19: Forecast error variance decomposition of interest rates - model with four global shocks



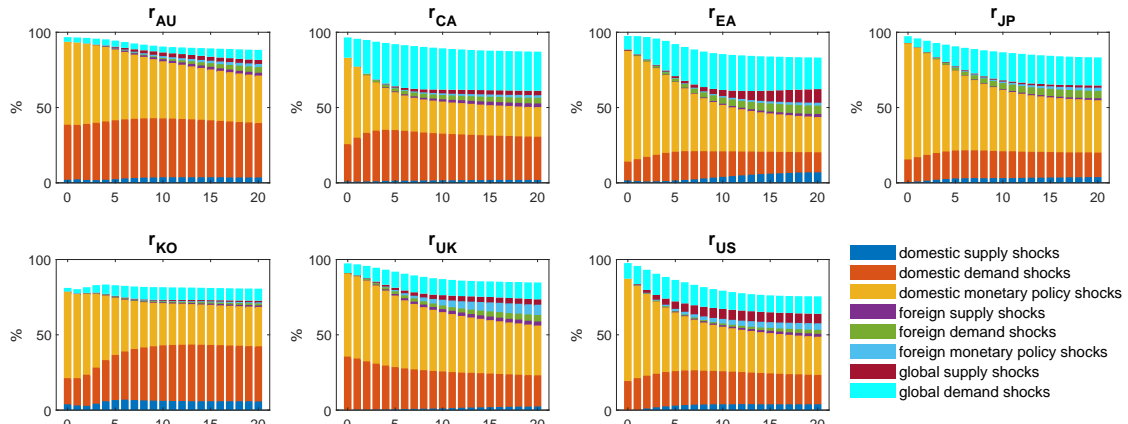
NOTES: The figure shows the forecast error variance decomposition of country-specific interest rates to domestic, foreign and global shocks over 20 quarters for the alternative model specification. Unlabeled shares are explained by the residual shock to the exchange rate equation.

Figure E.20: Forecast error variance decomposition of interest rates - model without trend



NOTES: The figure shows the forecast error variance decomposition of country-specific interest rates to domestic, foreign and global shocks over 20 quarters for the alternative model specification. Unlabeled shares are explained by the residual shock to the exchange rate equation.

Figure E.21: Forecast error variance decomposition of interest rates - model with 8 lags



NOTES: The figure shows the forecast error variance decomposition of country-specific interest rates to domestic, foreign and global shocks over 20 quarters for the alternative model specification. Unlabeled shares are explained by the residual shock to the exchange rate equation.

Figure E.22: Forecast error variance decomposition of interest rates - model with data starting in 1990:Q1

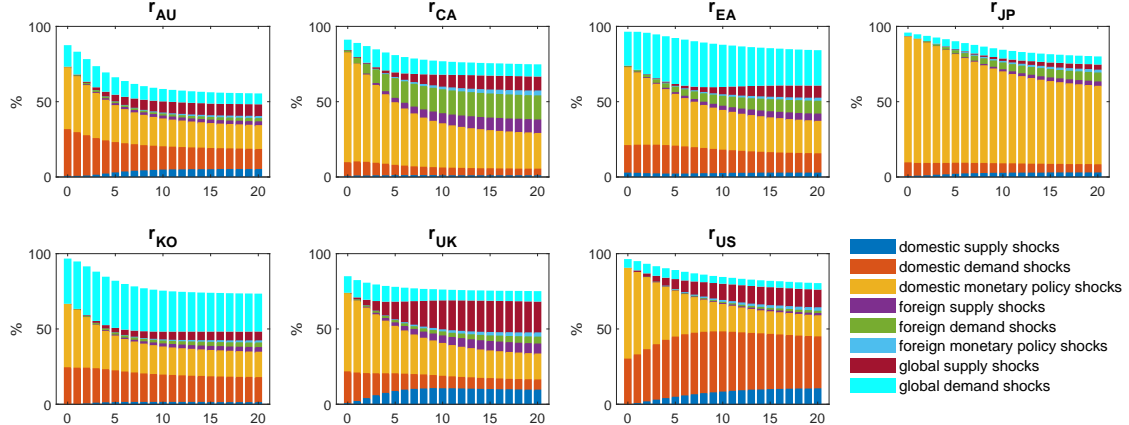


Figure E.23: Forecast error variance decomposition of interest rates - model with data ending in 2007:Q2

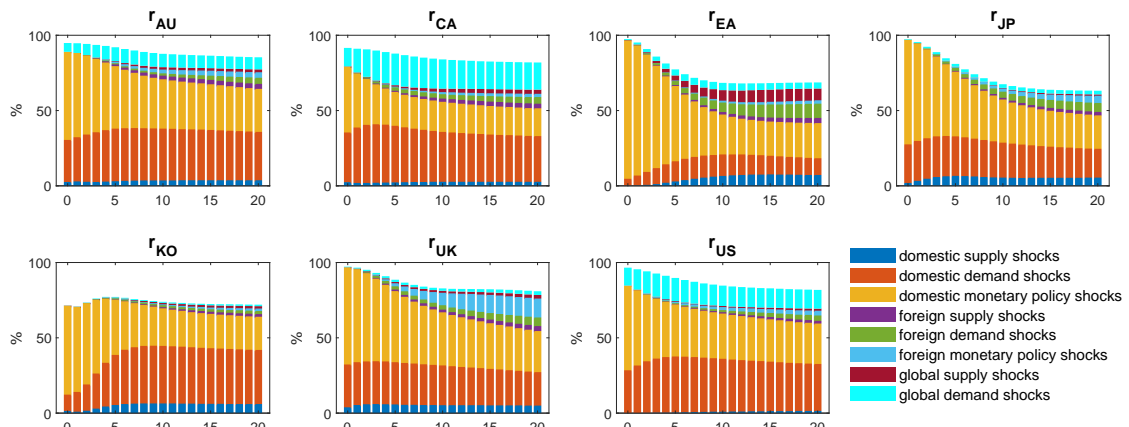
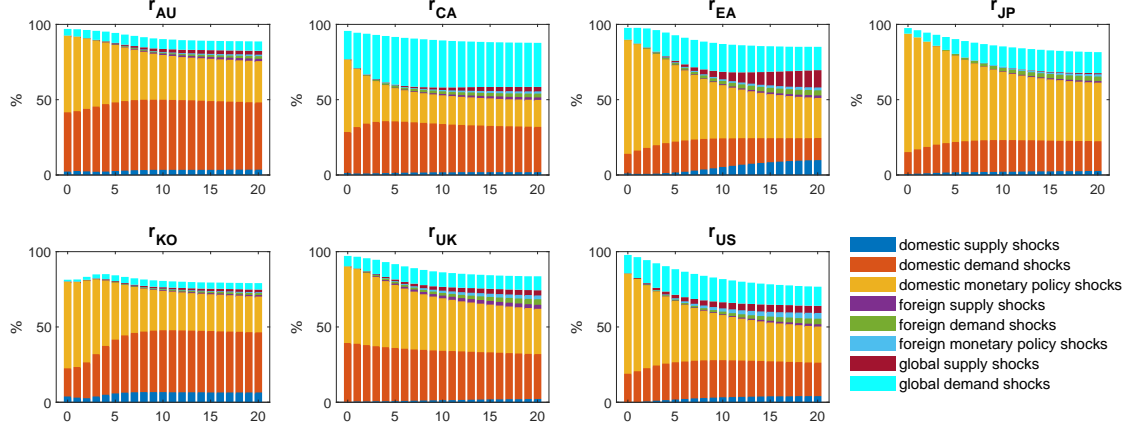
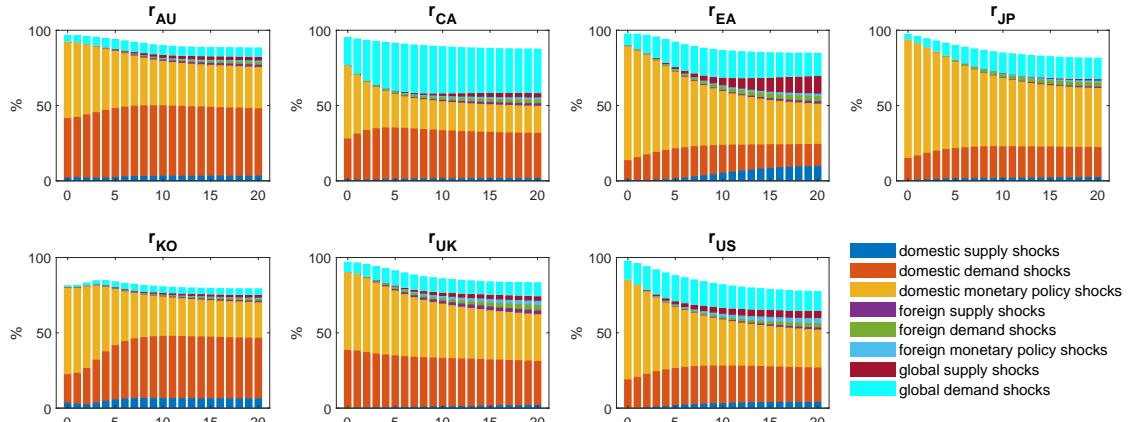


Figure E.24: Forecast error variance decomposition of interest rates - model with LBS liability weights



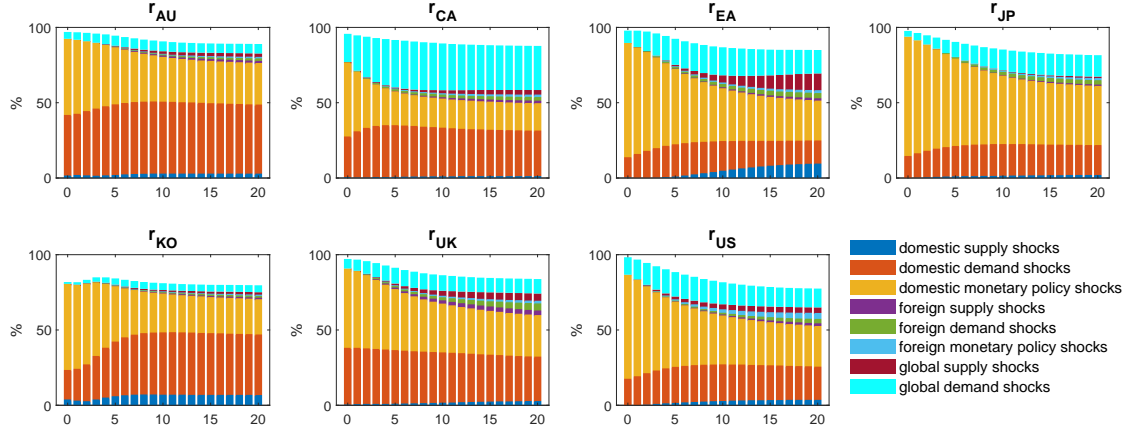
NOTES: The figure shows the forecast error variance decomposition of country-specific interest rates to domestic, foreign and global shocks over 20 quarters for the alternative model specification. Unlabeled shares are explained by the residual shock to the exchange rate equation.

Figure E.25: Forecast error variance decomposition of interest rates - model with LBS claim weights



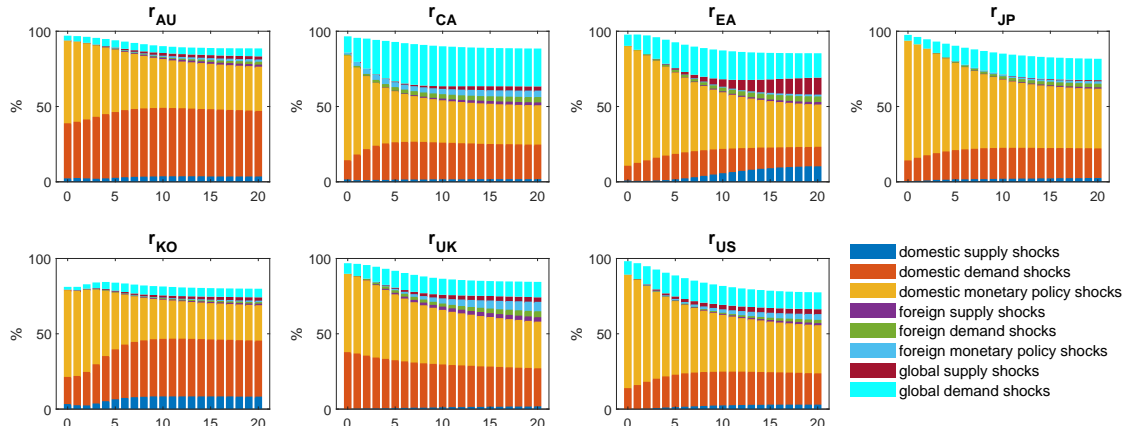
NOTES: The figure shows the forecast error variance decomposition of country-specific interest rates to domestic, foreign and global shocks over 20 quarters for the alternative model specification. Unlabeled shares are explained by the residual shock to the exchange rate equation.

Figure E.26: Forecast error variance decomposition of interest rates - model with CBS weights



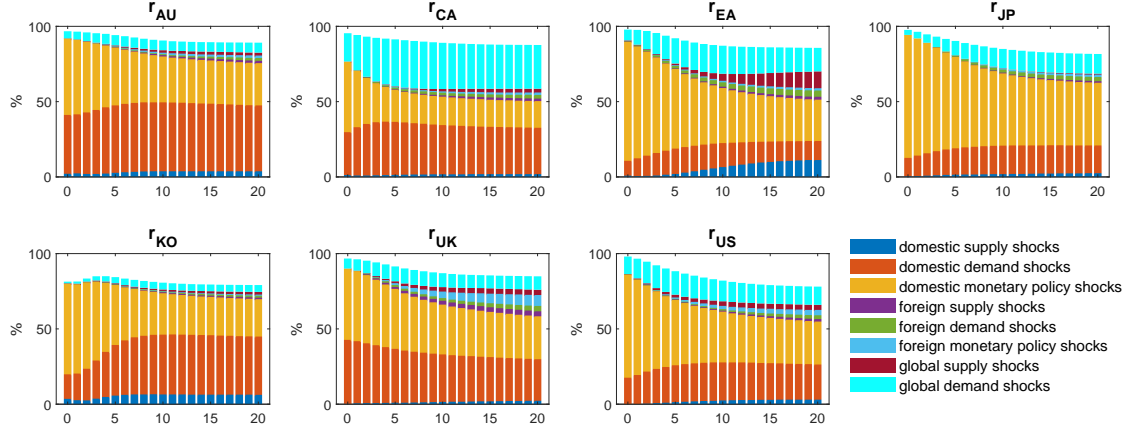
NOTES: The figure shows the forecast error variance decomposition of country-specific interest rates to domestic, foreign and global shocks over 20 quarters for the alternative model specification. Unlabeled shares are explained by the residual shock to the exchange rate equation.

Figure E.27: Forecast error variance decomposition of interest rates - model with foreign interest rates in the monetary policy rule



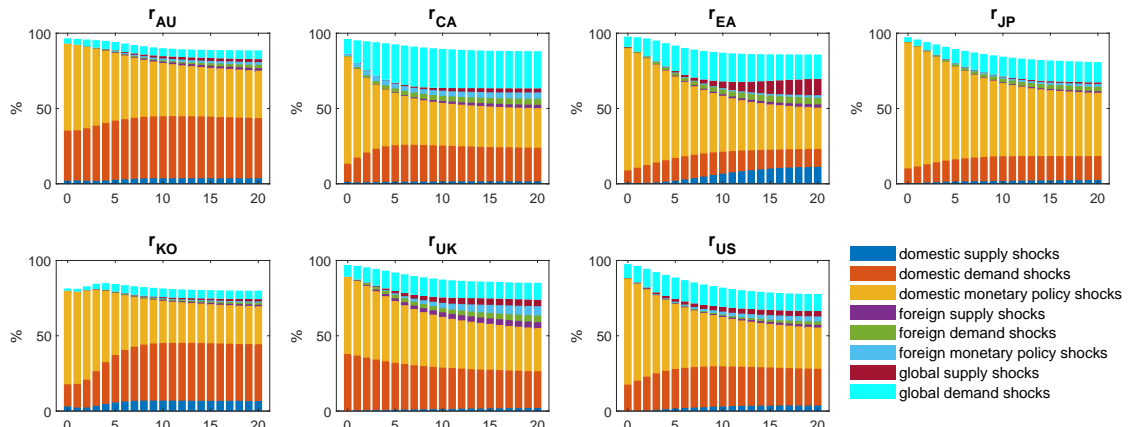
NOTES: The figure shows the forecast error variance decomposition of country-specific interest rates to domestic, foreign and global shocks over 20 quarters for the alternative model specification. Unlabeled shares are explained by the residual shock to the exchange rate equation.

Figure E.28: Forecast error variance decomposition of interest rates - model with foreign inflation in the monetary policy rule



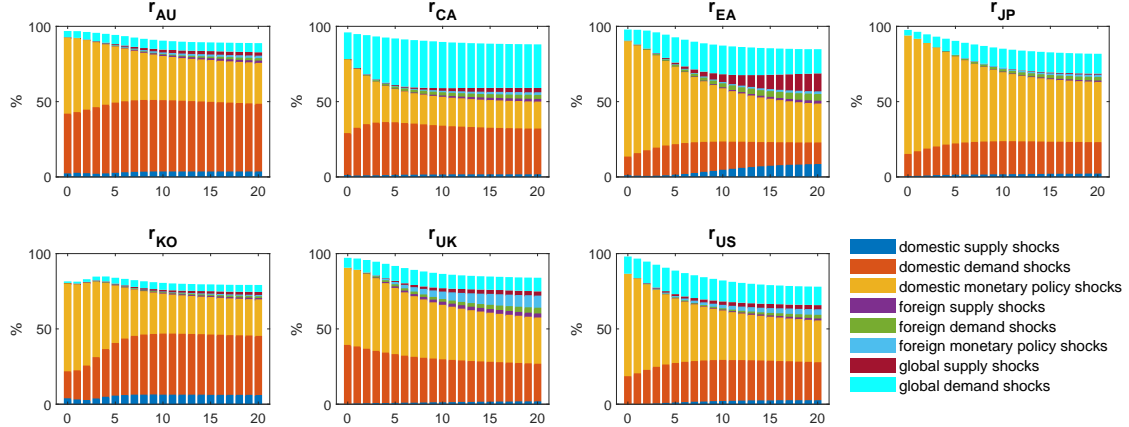
NOTES: The figure shows the forecast error variance decomposition of country-specific interest rates to domestic, foreign and global shocks over 20 quarters for the alternative model specification. Unlabeled shares are explained by the residual shock to the exchange rate equation.

Figure E.29: Forecast error variance decomposition of interest rates - model with foreign inflation and output gap in the monetary policy rule



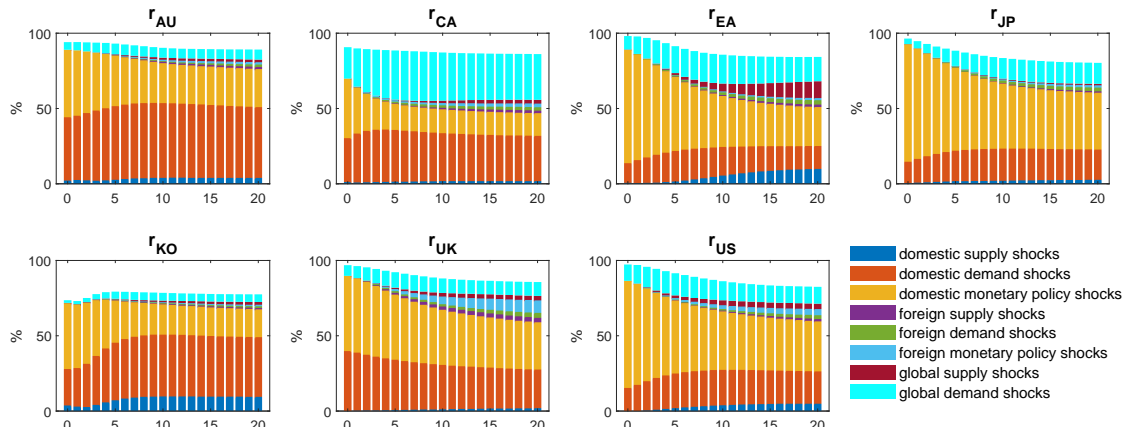
NOTES: The figure shows the forecast error variance decomposition of country-specific interest rates to domestic, foreign and global shocks over 20 quarters for the alternative model specification. Unlabeled shares are explained by the residual shock to the exchange rate equation.

Figure E.30: Forecast error variance decomposition of interest rates - model with foreign output gap in the supply equation



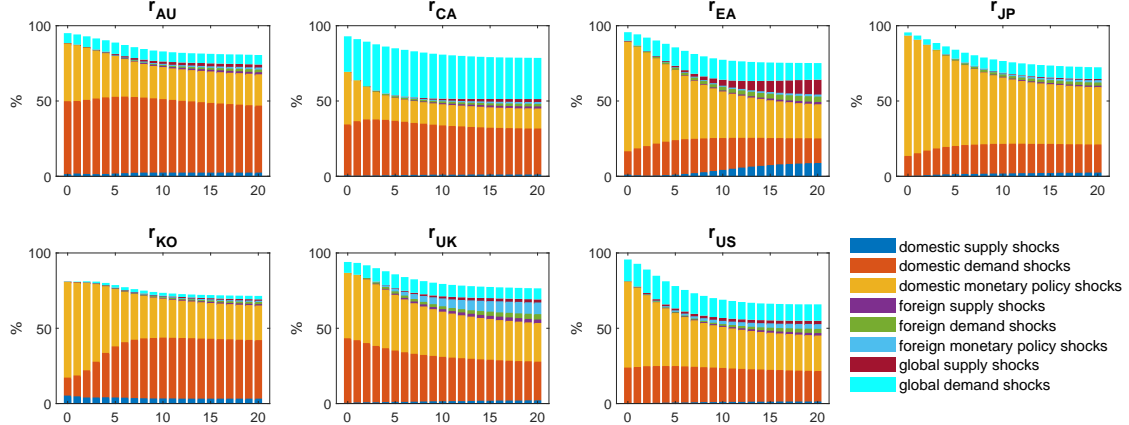
NOTES: The figure shows the forecast error variance decomposition of country-specific interest rates to domestic, foreign and global shocks over 20 quarters for the alternative model specification. Unlabeled shares are explained by the residual shock to the exchange rate equation.

Figure E.31: Forecast error variance decomposition of interest rates - model with interest rate differentials in exchange rate equation



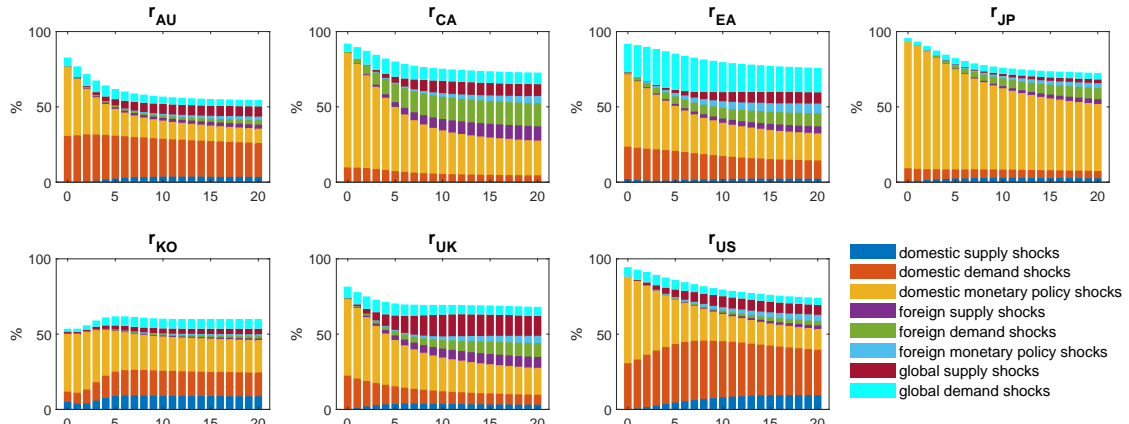
NOTES: The figure shows the forecast error variance decomposition of country-specific interest rates to domestic, foreign and global shocks over 20 quarters for the alternative model specification. Unlabeled shares are explained by the residual shock to the exchange rate equation.

Figure E.32: Forecast error variance decomposition of interest rates - model with stock prices



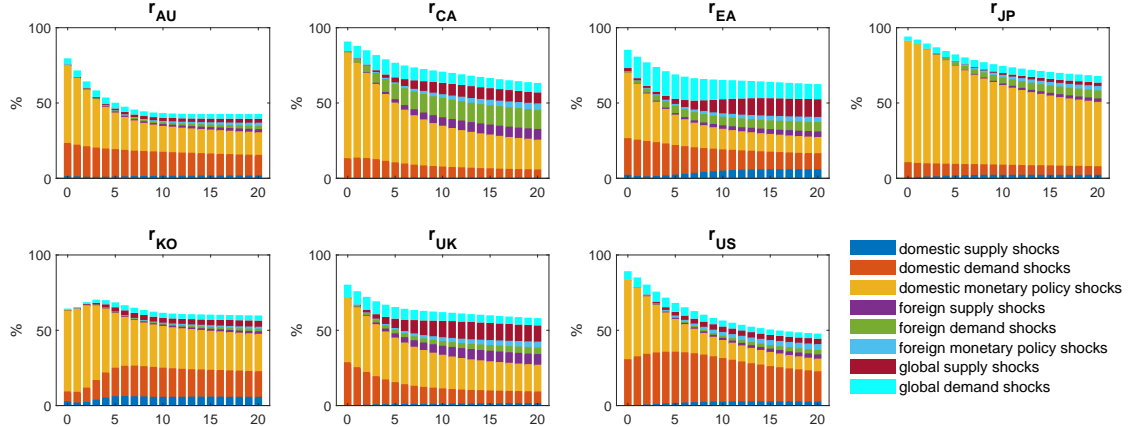
NOTES: The figure shows the forecast error variance decomposition of country-specific interest rates to domestic, foreign and global shocks over 20 quarters for the alternative model specification. Unlabeled shares are explained by the residual shock to the exchange rate equation and to the equation of the channel variable.

Figure E.33: Forecast error variance decomposition of interest rates - model with term spreads



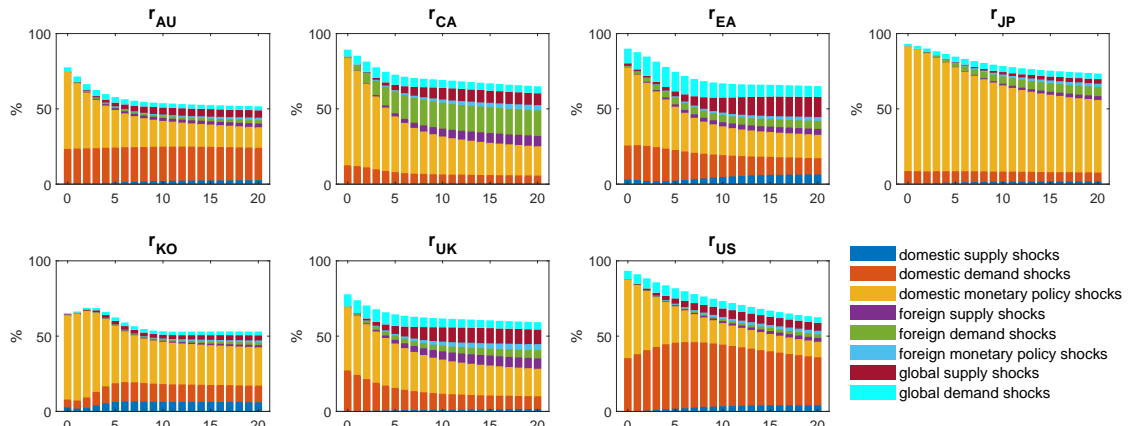
NOTES: The figure shows the forecast error variance decomposition of country-specific interest rates to domestic, foreign and global shocks over 20 quarters for the alternative model specification. Unlabeled shares are explained by the residual shock to the exchange rate equation and to the equation of the channel variable.

Figure E.34: Forecast error variance decomposition of interest rates - model with trade



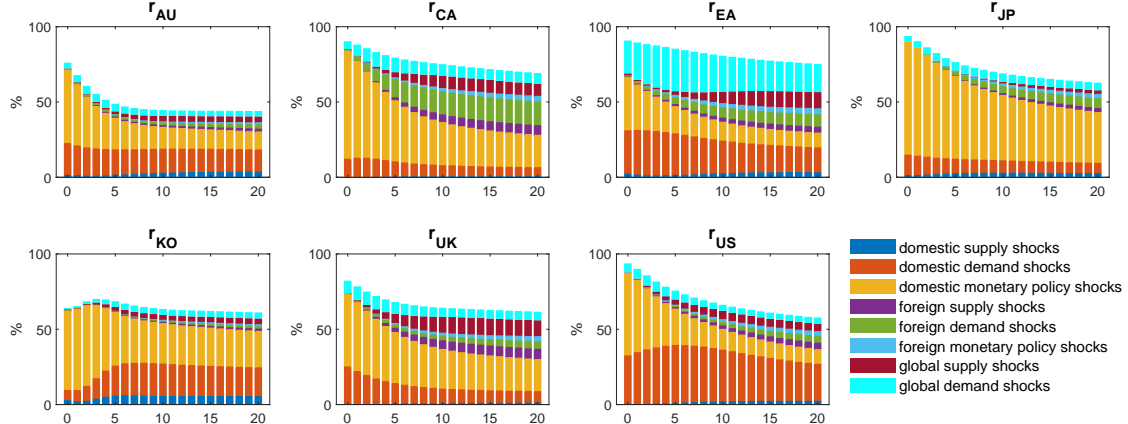
NOTES: The figure shows the forecast error variance decomposition of country-specific interest rates to domestic, foreign and global shocks over 20 quarters for the alternative model specification. Unlabeled shares are explained by the residual shock to the exchange rate equation and to the equation of the channel variable.

Figure E.35: Forecast error variance decomposition of interest rates - model with exports



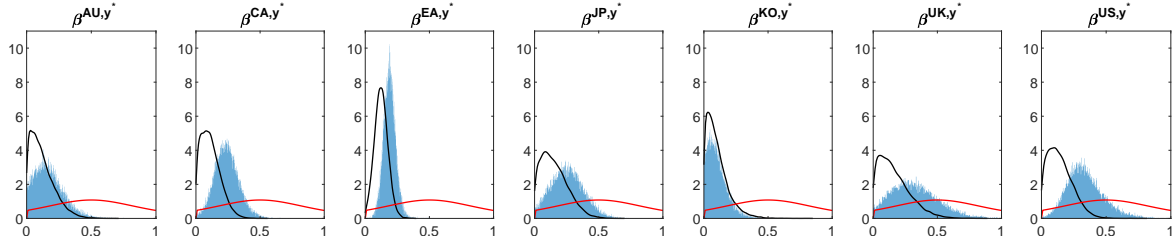
NOTES: The figure shows the forecast error variance decomposition of country-specific interest rates to domestic, foreign and global shocks over 20 quarters for the alternative model specification. Unlabeled shares are explained by the residual shock to the exchange rate equation and to the equation of the channel variable.

Figure E.36: Forecast error variance decomposition of interest rates - model with imports



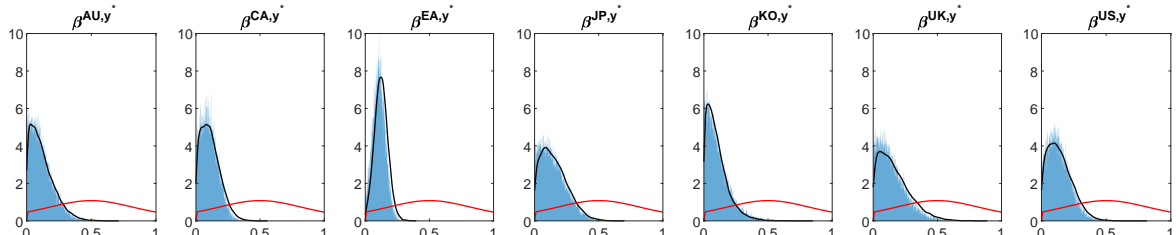
NOTES: The figure shows the forecast error variance decomposition of country-specific interest rates to domestic, foreign and global shocks over 20 quarters for the alternative model specification. Unlabeled shares are explained by the residual shock to the exchange rate equation and to the equation of the channel variable.

Figure E.37: Structural contemporaneous parameters β^{c,y^*} - model without global shocks



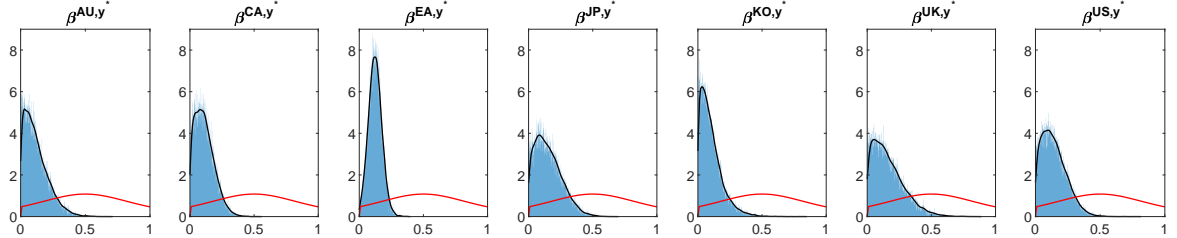
NOTES: The figure shows prior (red lines) and posterior distributions (histogram for the alternative model specification and black lines for baseline model) of the structural contemporaneous parameters.

Figure E.38: Structural contemporaneous parameters β^{c,y^*} - model with four global shocks



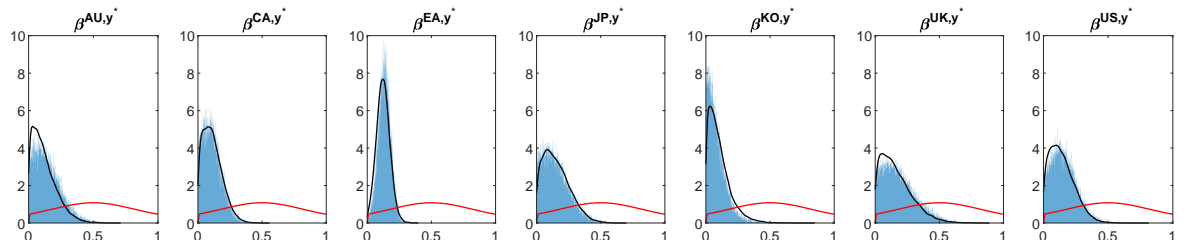
NOTES: The figure shows prior (red lines) and posterior distributions (histogram for the alternative model specification and black lines for baseline model) of the structural contemporaneous parameters.

Figure E.39: Structural contemporaneous parameters β^{c,y^*} - model without trend



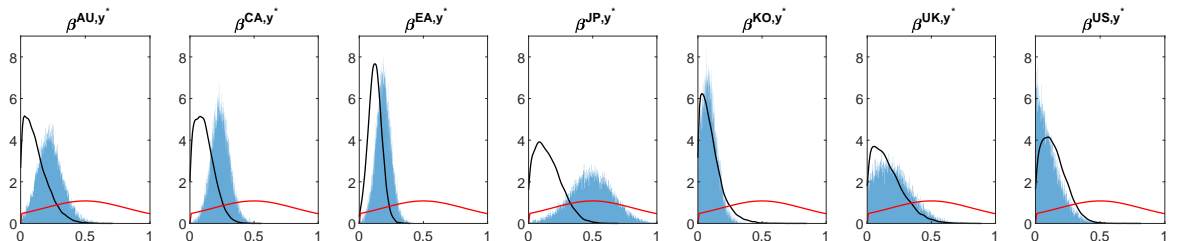
NOTES: The figure shows prior (red lines) and posterior distributions (histogram for the alternative model specification and black lines for baseline model) of the structural contemporaneous parameters.

Figure E.40: Structural contemporaneous parameters β^{c,y^*} - model with 8 lags



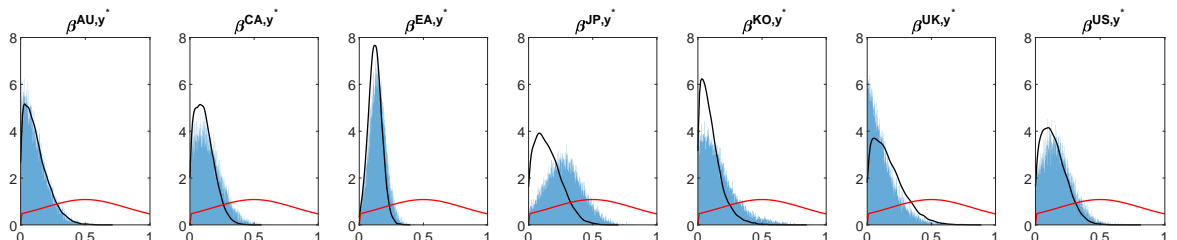
NOTES: The figure shows prior (red lines) and posterior distributions (histogram for the alternative model specification and black lines for baseline model) of the structural contemporaneous parameters.

Figure E.41: Structural contemporaneous parameters β^{c,y^*} - model with data starting in 1999:Q1



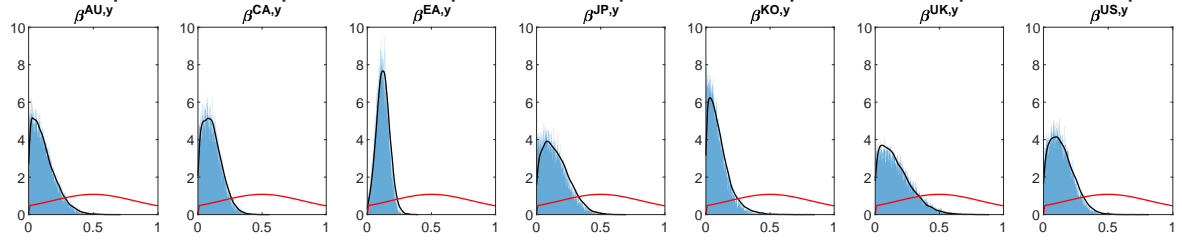
NOTES: The figure shows prior (red lines) and posterior distributions (histogram for the alternative model specification and black lines for baseline model) of the structural contemporaneous parameters.

Figure E.42: Structural contemporaneous parameters β^{c,y^*} - model with data ending in 2007:Q2



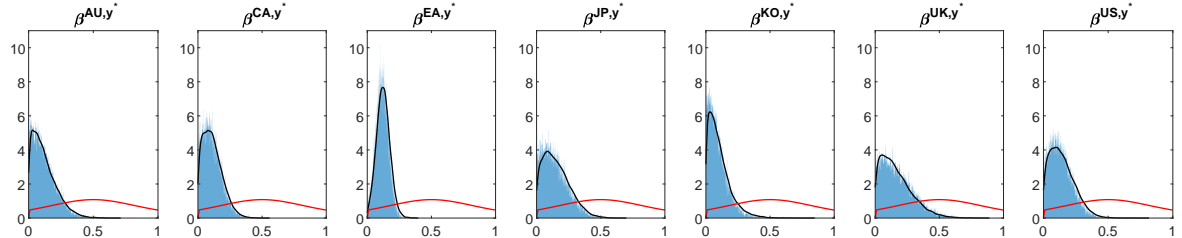
NOTES: The figure shows prior (red lines) and posterior distributions (histogram for the alternative model specification and black lines for baseline model) of the structural contemporaneous parameters.

Figure E.43: Structural contemporaneous parameters β^{c,y^*} - model with LBS liability weights



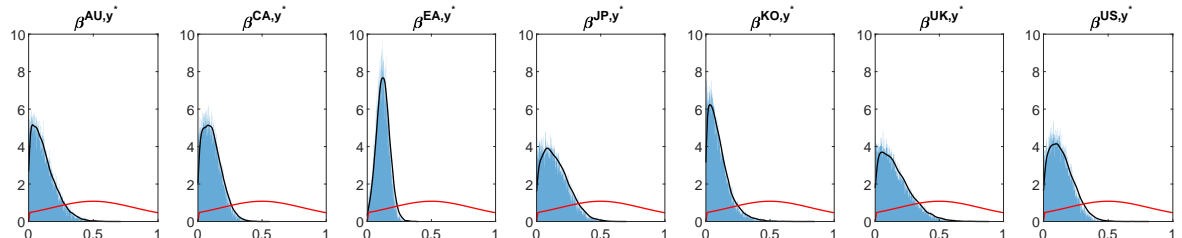
NOTES: The figure shows prior (red lines) and posterior distributions (histogram for the alternative model specification and black lines for baseline model) of the structural contemporaneous parameters.

Figure E.44: Structural contemporaneous parameters β^{c,y^*} - model with LBS claim weights



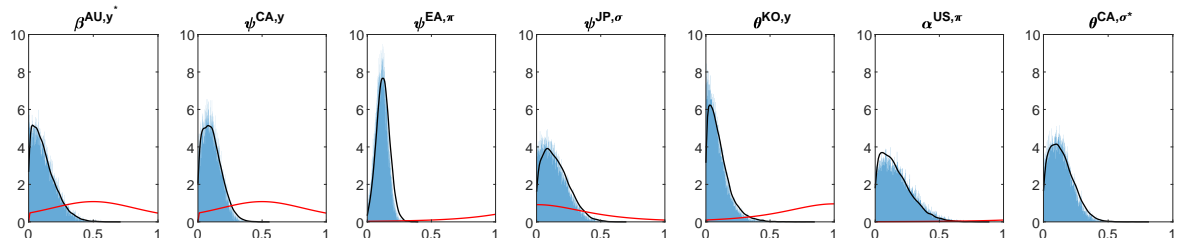
NOTES: The figure shows prior (red lines) and posterior distributions (histogram for the alternative model specification and black lines for baseline model) of the structural contemporaneous parameters.

Figure E.45: Structural contemporaneous parameters β^{c,y^*} - model with CBS weights



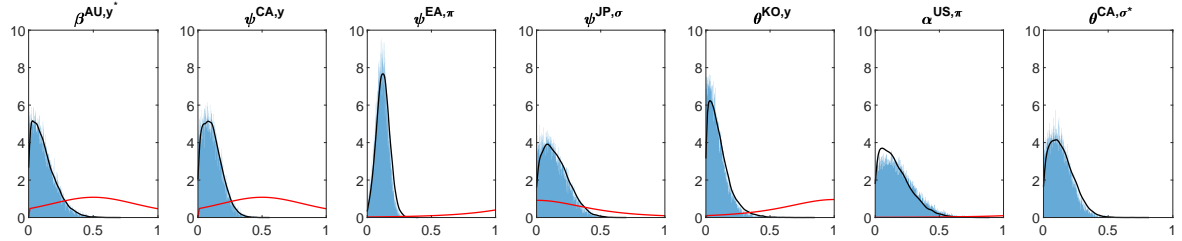
NOTES: The figure shows prior (red lines) and posterior distributions (histogram for the alternative model specification and black lines for baseline model) of the structural contemporaneous parameters.

Figure E.46: Structural contemporaneous parameters β^{c,y^*} - model with foreign interest rates in the monetary policy rule



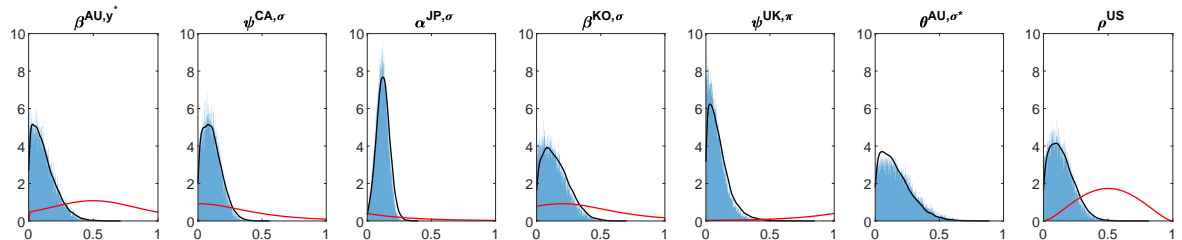
NOTES: The figure shows prior (red lines) and posterior distributions (histogram for the alternative model specification and black lines for baseline model) of the structural contemporaneous parameters.

Figure E.47: Structural contemporaneous parameters β^{c,y^*} - model with foreign inflation in the monetary policy rule



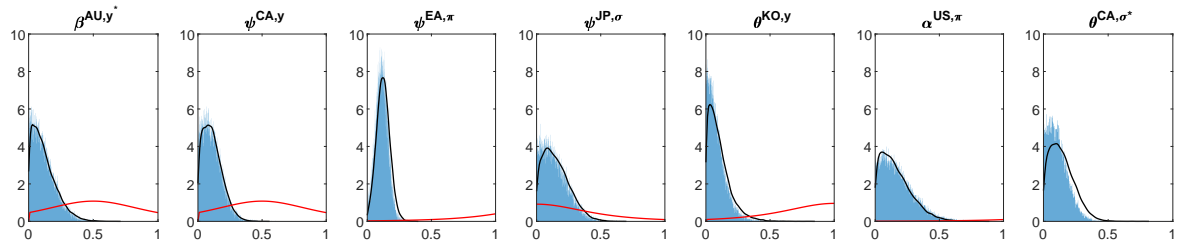
NOTES: The figure shows prior (red lines) and posterior distributions (histogram for the alternative model specification and black lines for baseline model) of the structural contemporaneous parameters.

Figure E.48: Structural contemporaneous parameters β^{c,y^*} - model with foreign inflation and output gap in the monetary policy rule



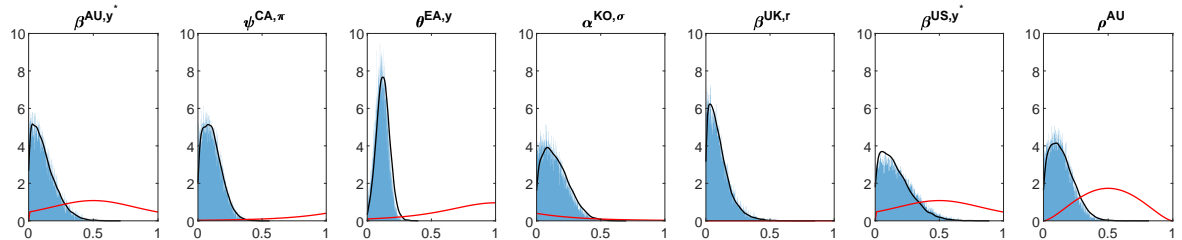
NOTES: The figure shows prior (red lines) and posterior distributions (histogram for the alternative model specification and black lines for baseline model) of the structural contemporaneous parameters.

Figure E.49: Structural contemporaneous parameters β^{c,y^*} - model with foreign output gap in the supply equation



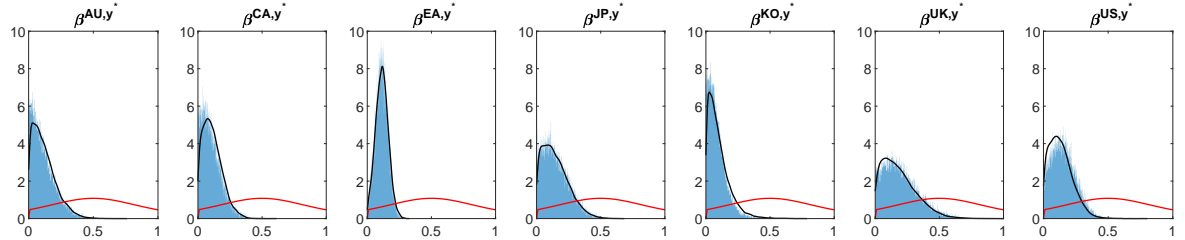
NOTES: The figure shows prior (red lines) and posterior distributions (histogram for the alternative model specification and black lines for baseline model) of the structural contemporaneous parameters.

Figure E.50: Structural contemporaneous parameters β^{c,y^*} - model with interest rate differentials in exchange rate equation



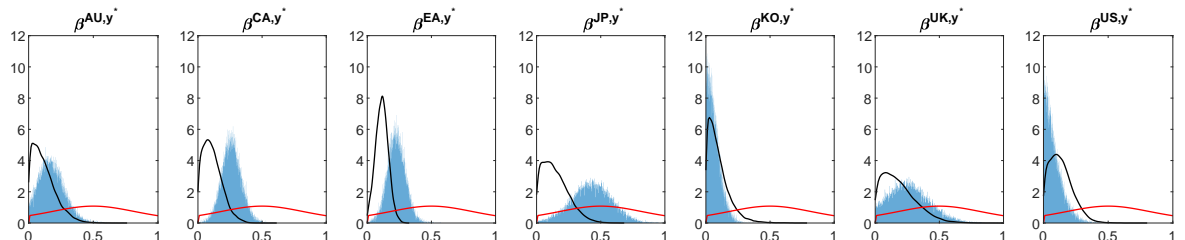
NOTES: The figure shows prior (red lines) and posterior distributions (histogram for the alternative model specification and black lines for baseline model) of the structural contemporaneous parameters.

Figure E.51: Structural contemporaneous parameters β^{c,y^*} - model with stock prices



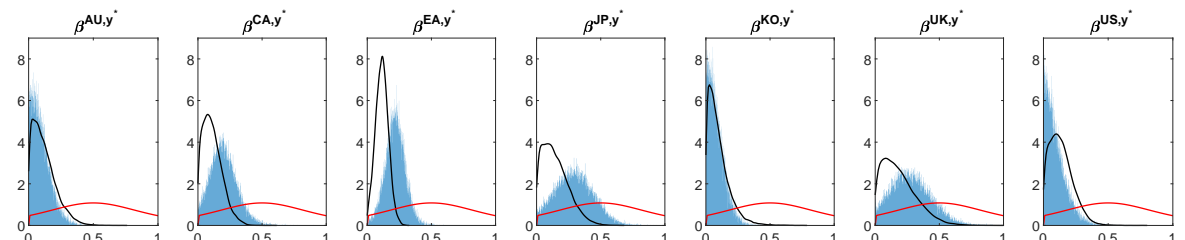
NOTES: The figure shows prior (red lines) and posterior distributions (histogram for the alternative model specification and black lines for baseline model) of the structural contemporaneous parameters.

Figure E.52: Structural contemporaneous parameters β^{c,y^*} - model with term spreads



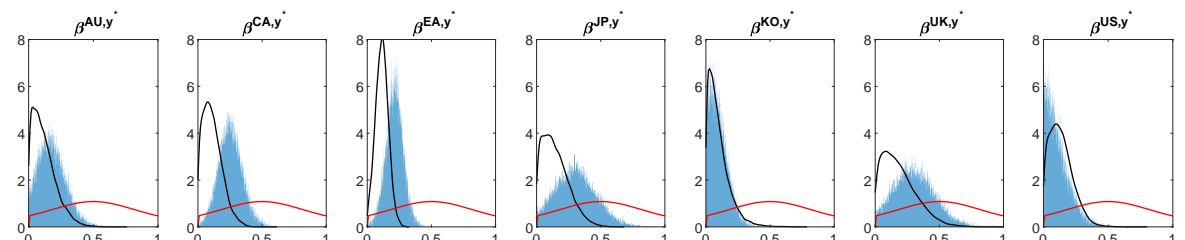
NOTES: The figure shows prior (red lines) and posterior distributions (histogram for the alternative model specification and black lines for baseline model) of the structural contemporaneous parameters.

Figure E.53: Structural contemporaneous parameters β^{c,y^*} - model with trade



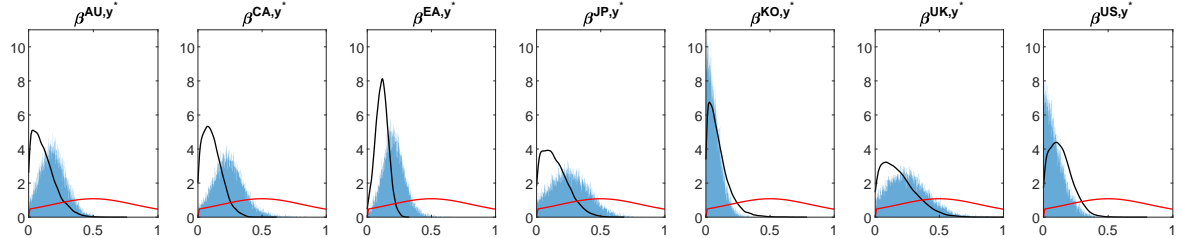
NOTES: The figure shows prior (red lines) and posterior distributions (histogram for the alternative model specification and black lines for baseline model) of the structural contemporaneous parameters.

Figure E.54: Structural contemporaneous parameters β^{c,y^*} - model with exports



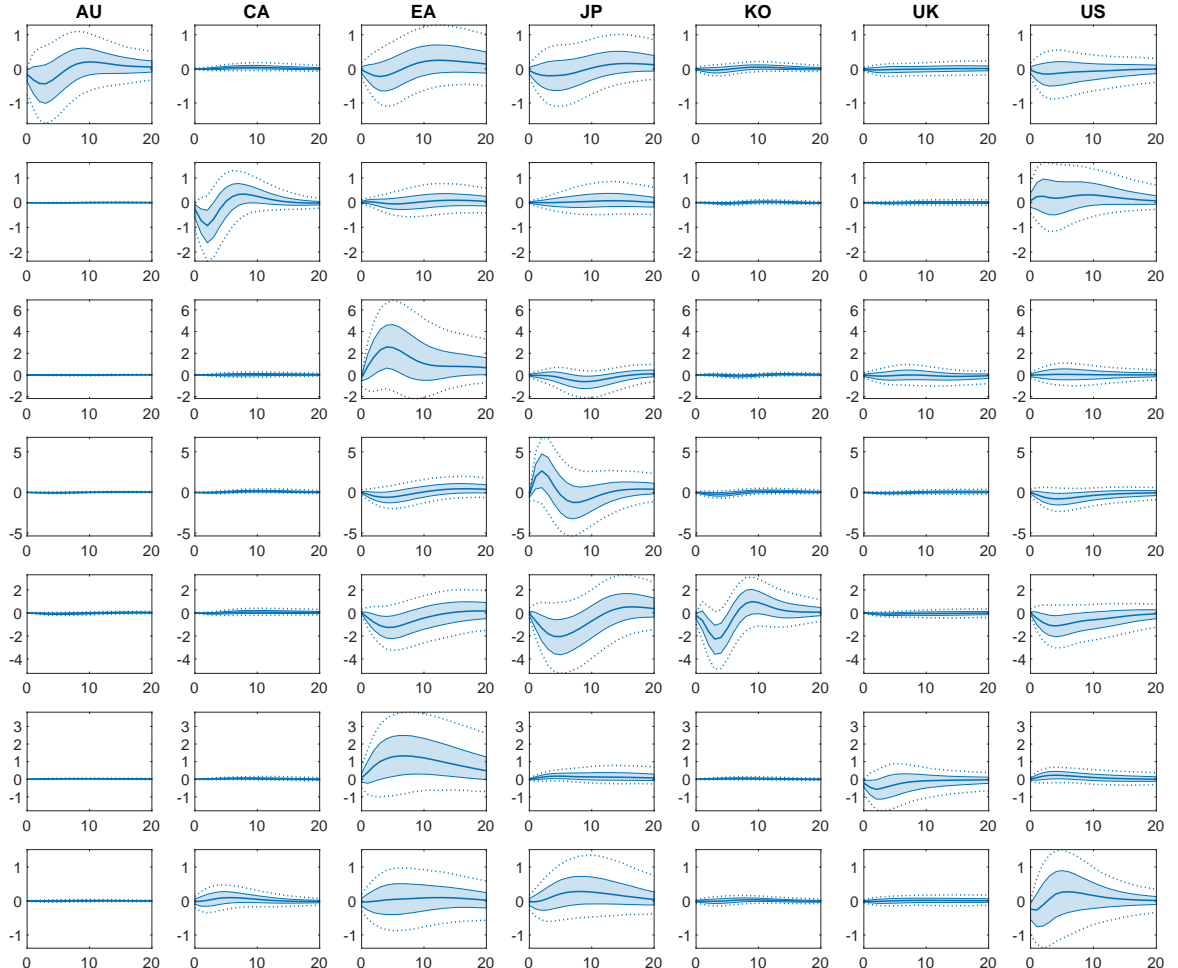
NOTES: The figure shows prior (red lines) and posterior distributions (histogram for the alternative model specification and black lines for baseline model) of the structural contemporaneous parameters.

Figure E.55: Structural contemporaneous parameters β^{c,y^*} - model with imports



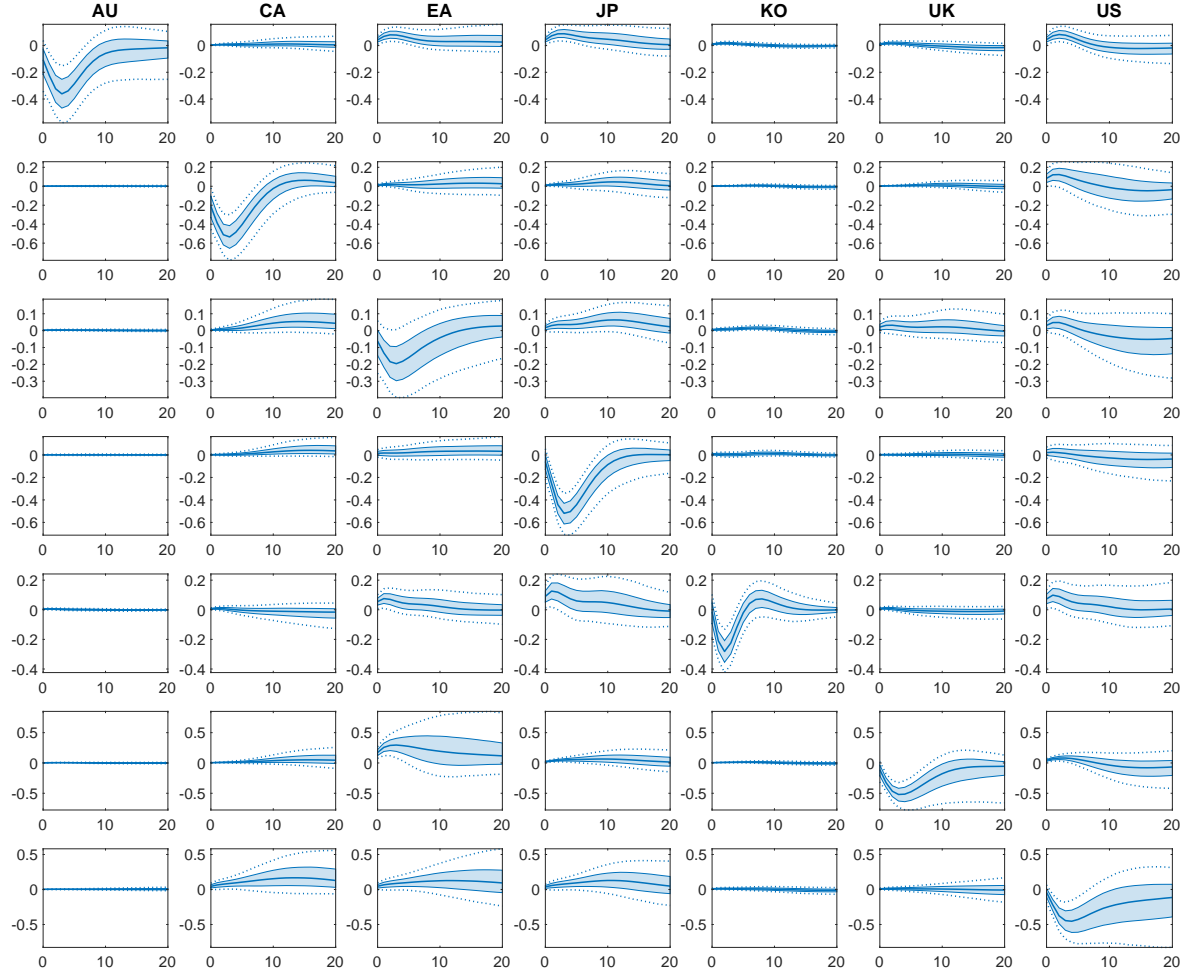
NOTES: The figure shows prior (red lines) and posterior distributions (histogram for the alternative model specification and black lines for baseline model) of the structural contemporaneous parameters.

Figure E.56: Impulse responses of stock prices to country-specific monetary policy shocks



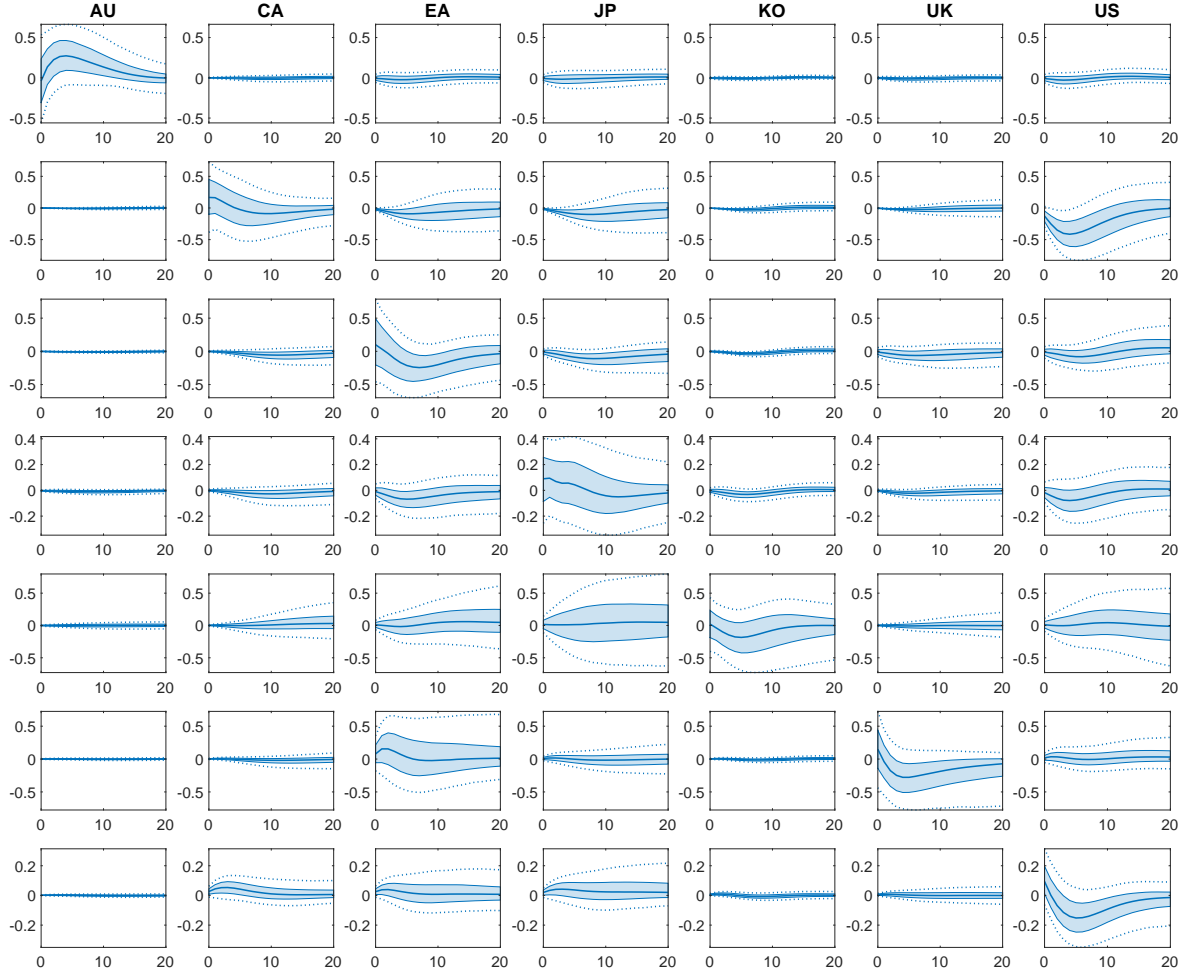
NOTES: The solid lines in the figure show median impulse responses of country-specific channel variable (in rows) to country-specific monetary policy shocks (in columns) over 20 quarters. The shaded areas (dotted lines) show the 68% (95%) posterior credibility sets. The shocks have size of one unit.

Figure E.57: Impulse responses of term spread to country-specific monetary policy shocks



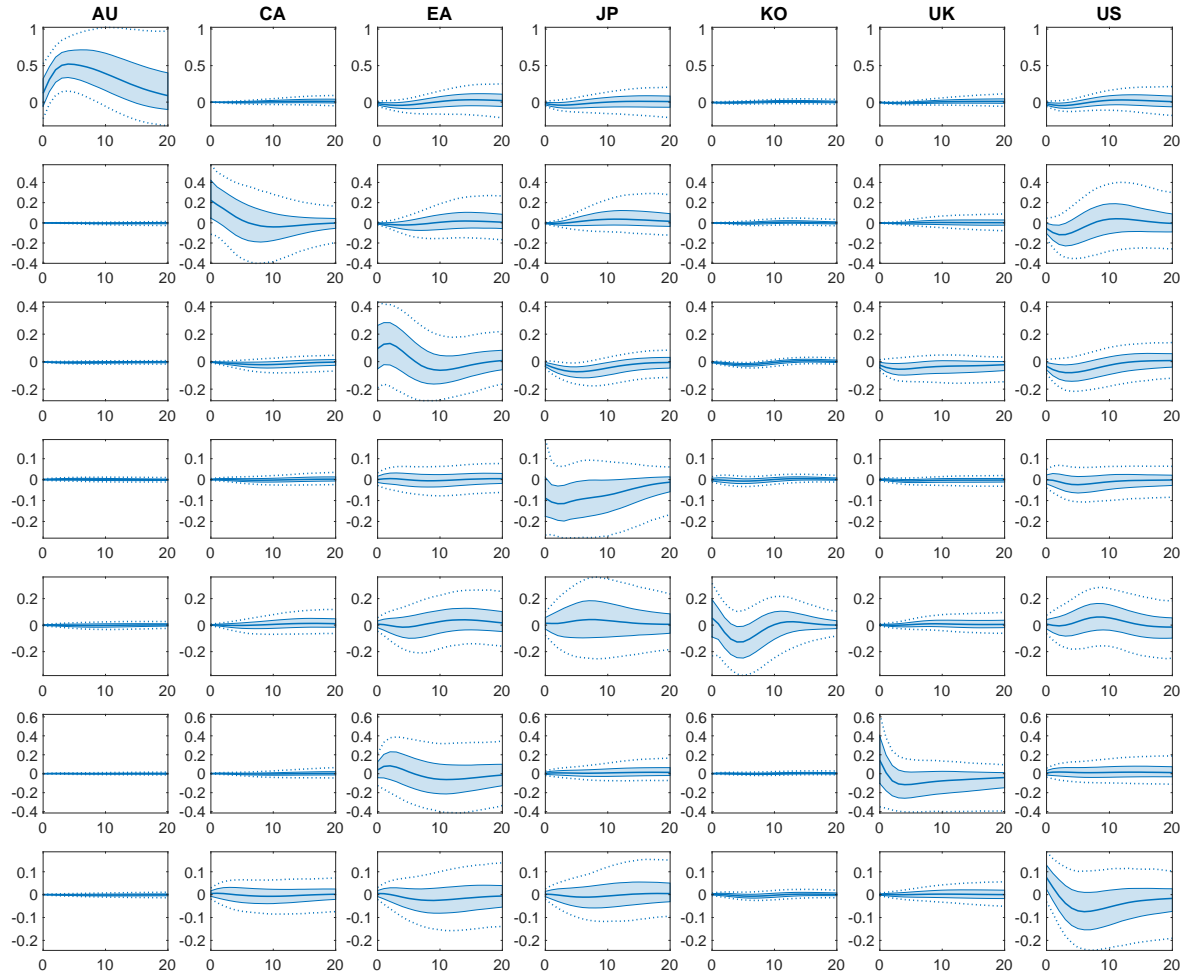
NOTES: The solid lines in the figure show median impulse responses of country-specific channel variable (in rows) to country-specific monetary policy shocks (in columns) over 20 quarters. The shaded areas (dotted lines) show the 68% (95%) posterior credibility sets. The shocks have size of one unit.

Figure E.58: Impulse responses of trade to country-specific monetary policy shocks



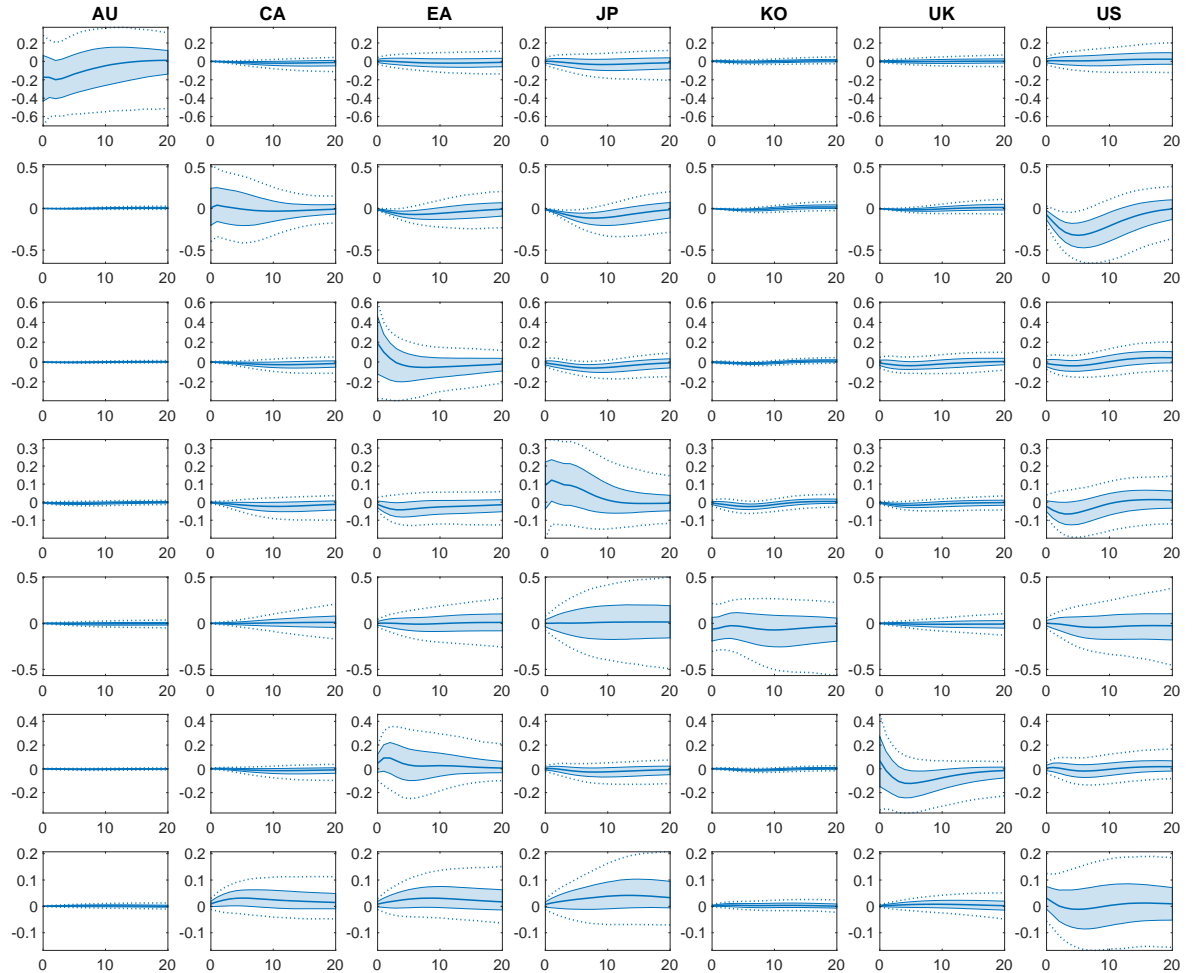
NOTES: The solid lines in the figure show median impulse responses of country-specific channel variable (in rows) to country-specific monetary policy shocks (in columns) over 20 quarters. The shaded areas (dotted lines) show the 68% (95%) posterior credibility sets. The shocks have size of one unit.

Figure E.59: Impulse responses of exports to country-specific monetary policy shocks



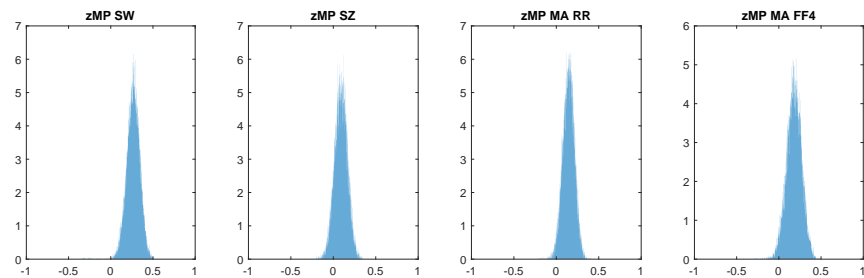
NOTES: The solid lines in the figure show median impulse responses of country-specific channel variable (in rows) to country-specific monetary policy shocks (in columns) over 20 quarters. The shaded areas (dotted lines) show the 68% (95%) posterior credibility sets. The shocks have size of one unit.

Figure E.60: Impulse responses of imports to country-specific monetary policy shocks



NOTES: The solid lines in the figure show median impulse responses of country-specific channel variable (in rows) to country-specific monetary policy shocks (in columns) over 20 quarters. The shaded areas (dotted lines) show the 68% (95%) posterior credibility sets. The shocks have size of one unit.

Figure E.61: Correlation of the global monetary policy shock in the model with four global shocks to instruments for US monetary policy shocks



NOTES: The histograms show the correlation of the posterior draws of the global monetary policy shock (from the model with one global shock for each economic equation) with various proxies for US monetary policy shocks from the literature, always multiplied such that the proxy is contractionary. SW: Bayesian DSGE of [Smets and Wouters \(2007\)](#), as used by [Stock and Watson \(2012\)](#); SZ: structural VAR of [Sims and Zha \(2006\)](#), as used by [Stock and Watson \(2012\)](#); MA RR: narrative Romer-Romer shocks from [Miranda-Agrippino and Rey \(2020\)](#); MA FF4: high-frequency shocks from [Miranda-Agrippino \(2016\)](#).

References

- Baumeister, C., Hamilton, J.D., 2015. Sign restrictions, structural vector autoregressions, and useful prior information. *Econometrica* 83, 1963–1999.
- Baumeister, C., Hamilton, J.D., 2018. Inference in structural vector autoregressions when the identifying assumptions are not fully believed: Re-evaluating the role of monetary policy in economic fluctuations. *Journal of Monetary Economics* 100, 48–65.
- Baumeister, C., Hamilton, J.D., 2019. Structural Interpretation of Vector Autoregressions with Incomplete Identification: Revisiting the Role of Oil Supply and Demand Shocks. *American Economic Review* 109, 1873–1910.
- Geweke, J., Zhou, G., 1996. Measuring the pricing error of the arbitrage pricing theory. *The Review of Financial Studies* 9, 557–587.
- Gilchrist, S., Zakrajšek, E., 2012. Credit spreads and business cycle fluctuations. *American Economic Review* 102, 1692–1720.
- Jermann, U., Quadrini, V., 2012. Macroeconomic effects of financial shocks. *American Economic Review* 102, 238–71.
- Käenzig, D.R., 2021. The Macroeconomic Effects of Oil Supply News: Evidence from OPEC Announcements. *American Economic Review* 111, 1092–1125.
- Lubik, T.A., Schorfheide, F., 2007. Do central banks respond to exchange rate movements? A structural investigation. *Journal of Monetary Economics* 54, 1069–1087.
- Miranda-Agrrippino, S., 2016. Unsurprising shocks: information, premia, and the monetary transmission. *Bank of England working papers* 626. Bank of England.
- Miranda-Agrrippino, S., Rey, H., 2020. US monetary policy and the global financial cycle. *The Review of Economic Studies* 87, 2754–2776.
- Mumtaz, H., Pinter, G., Theodoridis, K., 2018. What do VARs tell us about the impact of a credit supply shock? *International Economic Review* 59, 625–646.
- Sims, C.A., Zha, T., 2006. Were There Regime Switches in U.S. Monetary Policy? *American Economic Review* 96, 54–81.
- Smets, F., Wouters, R., 2007. Shocks and frictions in us business cycles: A bayesian dsge approach. *American economic review* 97, 586–606.
- Stock, J.H., Watson, M.W., 2012. Disentangling the channels of the 2007-09 recession. *Brookings Papers on Economic Activity* 43, 81–156.